1 **Title:**   The effects of weak selection on neutral diversity at linked sites

2

3 **Author:** Brian Charlesworth

4

5 **Affiliation:**

6 Institute of Evolutionary Biology, School of Biological Sciences, University of Edinburgh,

7 Edinburgh EH9 3FL, United Kingdom

8

9 **Key words:** Associative overdominance, background selection, fixation times, loss times,

10 neutral variability

11

12 **Running title:** Weak selection and genetic diversity

13

14

15 **Corresponding author:**

16   *Name:* Brian Charlesworth

17   *Address:* Institute of Evolutionary Biology, School of Biological Sciences, Ashworth

18   Laboratories, University of Edinburgh, King's Buildings, Charlotte Auerbach Road,

19   Edinburgh EH9 3FL, UK

20   *Telephone:* +44 131 650 5751

21   *Email:* Brian.Charlesworth@ed.ac.uk

22
23

24   **Abstract**

25

26   The effects of selection on variability at linked sites have an important influence on

27   levels and patterns of within-population variation across the genome. Most theoretical

28   models of these effects have assumed that selection is sufficiently strong that allele

29   frequency changes at the loci concerned are largely deterministic. These models have

30   led to the conclusion that directional selection for new selectively favorable mutations,

31   or against recurrent deleterious mutations, reduces nucleotide site diversity at linked

32   neutral sites. Recent work has shown, however, that fixations of weakly selected

33   mutations, accompanied by significant stochastic changes in allele frequencies, can

34   sometimes cause higher diversity at linked sites when compared with the effects of

35   fixations of neutral mutations. The present paper extends this work by deriving

36   approximate expressions for the mean times to loss and fixation of mutations subject to

37   selection, and analysing the conditions under which selection increases rather than

38   reduces these times. Simulations are used to examine the relations diversity at a neutral

39   site and the fixation and loss times of mutations at a linked site subject to selection. It is

40   shown that the long-term level of neutral diversity can be increased over the equilibrium

41   expectation in the absence of selection by recurrent fixations and losses of linked,

42   weakly selected dominant or partially dominant favorable mutations, and by linked

43   recessive or partially recessive deleterious mutations. The results are used to examine

44   the conditions under which associative overdominance, as opposed to background

45   selection, is likely to operate.

46

47

Introduction

There is now a large body of data showing that the levels of within-population DNA sequence diversity across the genomes of many organisms are significantly affected by the effects of selection on sites linked to those under observation, especially in genomic regions or species where recombination rates are low; for recent reviews, see Cutter and Payseur (2013) and Charlesworth and Jensen (2021). Interpretations of these observations have mainly focussed on reductions in variation at linked neutral or nearly neutral sites caused by the spread of selectively favorable variants (selective sweeps), or the elimination of rare, deleterious mutations (background selection or BGS). The population genetic models used to describe these processes usually assume that selection is sufficiently strong in relation to genetic drift that deterministic equations are sufficient to describe the behavior of the sites under selection, except for the initial and final periods of the fixation of beneficial mutations (reviewed by Charlesworth and Jensen 2021).

Interest has, however, recently been revived in the process known as associative overdominance (Frydenberg 1963; Sved 1968; Ohta 1971; Latter 1998; Pamilo and Palsson 1998, 1999; Wang and Hill 1999; Zhao and Charlesworth 2016; Waller 2021), whereby the level of diversity at a neutral locus in a diploid population can be enhanced by the presence of linked deleterious alleles maintained by mutation pressure. Recent theoretical work has shown that this can happen when the deleterious alleles concerned are sufficiently recessive, and selection is sufficiently weak in relation to drift (Zhao and Charlesworth 2016). The latter condition requires the product of the effective size of the population (N_e) and the selection coefficient against homozygotes for a mutation (s) to be the order of 1 or less, consistent with previous results from computer simulations (Latter 1998; Palsson and Pamilo 1999; Wang and Hill 1999). There is evidence for the operation of associative overdominance (AOD) in both small populations (Latter 1998; Zhao and Charlesworth 2016; Schou et al. 2017; Waller 2021), and in genomic regions with low recombination, where N_e is reduced as a result of background selection and selective sweeps (Becher et al. 2020; Gilbert et al. 2020). In contrast, if the effects of drift on the frequencies of deleterious alleles are negligible, background selection (BGS) operates, causing a reduction in variability at linked sites (Charlesworth et al. 1993; Hudson and Kaplan 1995; Nordborg et al. 1996).

Under conditions where AOD is acting, deleterious variants at sites under selection are likely to become fixed as a result of drift, and reverse mutations that increase fitness can eventually arise and replace them as a result of the joint effects of drift and selection. In the long term, a population that is constant in size will reach a statistical equilibrium under the joint effects of drift,

81 mutation and selection, a situation that is similar to that envisaged in the Li-Bulmer model of the

82 evolution of codon usage bias, which assumes a constant flux of fixations of favorable and

83 beneficial mutations at sites under selection (Li 1987; Bulmer 1991; McVean and Charlesworth

84 1999). In order to understand the effects of AOD, it is therefore important to have a model of the

85 effects of this flux on variability at linked neutral sites.

86 A basis for such a model is provided by the results of Mafessoni and Lachmann (2015) on

87 the expected times to fixation and loss of new autosomal mutations in a randomly mating

88 population, and on the effects of fixation events on the patterns of variability at linked neutral loci.

89 They showed that a weakly selected ($N_e s$ of order 1), favorable mutation destined for fixation can

90 have a longer mean time to fixation or loss than a neutral mutation, provided that it is dominant or

91 partially dominant. The same applies to weakly selected, partially recessive deleterious mutations.

92 Furthermore, the fixation of a dominant or partially dominant favorable mutation, or a recessive or

93 partially recessive deleterious mutation, can enhance variability at a linked neutral site compared

94 with the effect of fixation of a neutral variant, although variability is still lower than in an

95 equilibrium population without any selection. These conclusions have been confirmed in

96 simulations described by Johri *et al.* (2021); similar situations where fitnesses fluctuate over time

97 have been studied by Kaushik and Jain (2021). As pointed out by Charlesworth and Jensen (2021),

98 these results are relevant to the analysis of AOD by Zhao and Charlesworth (2016), who showed

99 that a neutral locus closely linked to a locus subject to mutation to deleterious alleles can lose

100 variability more slowly than in the absence of selection, provided that the mutations are recessive or

101 partially recessive and selection is sufficiently weak relative to the effects of genetic drift.

102 The purpose of this paper is to obtain approximate analytical expressions for the expected

103 sojourn times of new mutations for the case of weak selection, and to use these to illuminate the

104 results of Mafessoni and Lachmann (2015) on the fixation and loss of weakly selected mutations.

105 Computer simulations are used in conjunction with these results to examine the effects of fixation

106 and loss of weakly selected mutations on variability at linked neutral sites. The results are used to

107 develop a semi-analytical model of AOD for the case of statistical equilibrium between mutation,

108 selection and drift. They also provide a new way of describing BGS, when applied to situations

109 when selection is so strong in relation to drift, so that deleterious mutations have a negligible

110 chance of becoming fixed in the population. The focus is on the case when there is no

111 recombination between neutral and selected sites, since this gives the clearest signal and allows the

112 causes of the observed patterns to be analysed without the complications introduced by

113 recombination.

114

Material and methods

Simulation methods

To check the accuracy of the diffusion equation results for expected times to fixation or loss (see the section *Theoretical Results*), a biallelic autosomal locus in a Wright-Fisher population with constant size N was modeled, implying that the effective population size N_e is equal to N. For a given simulation run, a single A_2 allele was introduced into the population that was fixed for its alternative allele A_1 The mutant allele could be either selectively favorable or deleterious. The expected change in the frequency x of A_2 in a given generation for an assigned selection model was calculated using the standard discrete-generation selection formulation (for details of the model of selection, see the section *Theoretical Results, Approximate times to fixation and loss of a new mutation*). Binomial sampling using the frequency of A_2 after selection and $2N$ as parameters was used to obtain the value of x in the next generation. Large numbers of replicate simulations were run in order to obtain the mean times to fixation and loss of A_2, conditioned on its fixation or loss, respectively.

This procedure was modified in order to calculate the effects of a sweep on pairwise diversity at a neutral locus with an arbitrary degree of linkage to the selected locus. As described in Charlesworth (2020a) and Johri et al. (2021), the algorithm of Tajima (1990) was used to calculate the effects of a sweep on pairwise diversity at a neutral locus with an arbitrary degree of linkage to a selected locus with two alleles, A_1 and A_2. Tajima's Equations (27) provide three coupled, forward-in-time recurrence relations for the expected diversities at the neutral locus for pairs of haplotypes carrying either A_1 or A_2, and the divergence between A_1 and A_2 haplotypes. These are conditioned on a given generation-by-generation trajectory of allele frequencies at the selected locus, assuming the infinite sites model of mutation and drift (Kimura 1971). In the present study, there is interest in the effects of both losses and fixations of either deleterious or advantageous A_2 mutations on diversity statistics over the time-course leading to loss or fixation of A_2, whereas the previous studies only considered the effects of fixations.

For a given simulation run, a single A_2 allele was introduced into the population, with zero expected pairwise diversity at the associated neutral locus. The initial expected pairwise diversity among A_1 alleles and divergence between A_1 and A_2 were set equal to those for an equilibrium population in the absence of selection, $\theta = 4N_e\mu$, where μ is the neutral mutation rate. Since only diversities relative to θ are of interest here, θ was set to 0.001 in order to satisfy the infinite sites assumption. Equations (27) of Tajima (1990) were applied to the previous value of the allele frequency in order to obtain the state of the neutral locus in the new generation.

148   The simulation procedure for selection and drift at the selected locus was repeated

149 generation by generation until A_2 was lost or fixed; if the effect of loss on diversity at the neutral

150 locus was of interest, only runs in which A_2 was lost were retained, and the value of the pairwise

151 diversity among A_2 alleles at the time of its loss was determined. Similarly, the effects of

152 fixations were studied by recording the properties of runs in which A_2 was fixed. Large numbers

153 of replicate simulations were used (between 10^4 and 10^6, depending on the parameter values),

154 because there is a large amount of variation in the values of the population statistics between

155 replicate runs.

156   Diversity statistics were obtained in each generation for the three genotypes at the

157 selected locus. They were measured relative to the equilibrium neutral values, and were thus

158 equivalent to the mean coalescent times on the timescale of $2N_e$ generations. The sums of the

159 pairwise diversity statistics were taken over the whole time course of a loss or fixation, for A_1

160 versus A_1, A_1 versus A_2, and A_2 versus A_2 haplotypes, as well as the mean over all three of these

161 comparisons, weighted by their frequencies in the generation in question. In addition, the neutral

162 diversity of fixed haplotypes at the time of loss or fixation of the mutation was determined.

163

164 **Numerical integrations**

165 The notation and results described in Ewens (2004, Chapters 4 and 5) are used here, with some

166 slight modifications. The diffusion equation expressions shown in the Appendix yield the sojourn

167 time densities at frequency x of A_2 given an initial frequency $q,$ which are denoted by $t^*(x, q)$ and

168 $t^{**}(x, q)$ for fixations and losses, respectively (see Equations A1 and A6). The mean times spent

169 between frequencies x and $x + dx$ are given by $t^*(x, q)\, dx$ and $t^{**}(x, q)\, dx,$ respectively, where dx

170 is an arbitrarily small increment in x. The sojourn time densities involve integrals of the

171 function $\psi(y)$, defined by Equation (A1c). For a given value of x, these integrals can be evaluated

172 for specified upper and lower values of y by using the series expansions in Equations (A3). The

173 simplest way to obtain the corresponding mean times to fixation and loss, t^* and t^{**}, for a new

174 mutation with a haploid population size N_H (see next section) is to sum the products $t^*(x, q)\, /N_H$

175 and $t^{**}(x, q)/N_H$ over all values of x between q and 1, with $q = 1/N_H$ (Ewens 2004, p.142).

176

177 **Theoretical results**

178 **Approximate expected times to fixation and loss of a new mutation**

179 A more general model of selection than that used by Mafessoni and Lachmann (2015) is employed

180 here, using the notation of Charlesworth (2020a,b). A biallelic locus in a discrete generation,

181   panmictic population is assumed, with frequencies x and $1 - x$ in a given generation of alleles A_2

182   and A_1, respectively; the population is initially fixed for A_1. The new mutation, A_2, is introduced as

183   a single copy. To accommodate a general genetic system, the number of haploid genomes at a locus

184   that are present in the population is denoted by N_H, so that the initial frequency of A_2 is $q = 1/N_H$

185   (Charlesworth 2020a). Selection is sufficiently weak that second-order terms in the selection

186   coefficient s for A_2A_2 homozygotes can be neglected (s is negative if A_2A_2 individuals are at a

187   selective disadvantage); $1 + s$ is the fitness of A_2A_2 relative to the fitness of A_1A_1. The effective

188   population size is N_e; time is measured in units of the coalescent time, $2N_e$ generations. The scaled

189   selection coefficient is defined as $\gamma = 2N_e s$. Under these assumptions, the rate of change in

190   frequency A_2 can be written as:

191

192 $$\Delta x \approx x(1 - x)\gamma(a + bx) \qquad\qquad (1)$$

193

194   where the coefficients a and b depend on the genetic system and breeding system, and higher-order

195   in s having been neglected (Charlesworth 2020a). In the case of an autosomal locus with random

196   mating, $a = h$ and $b = 1 - 2h$. Here, h is the dominance coefficient, such that the fitness of A_1A_2

197   heterozygotes relative to that of A_1A_1 homozygotes is equal to $1 + hs$. This familiar case will be the

198   focus of this study, but the conclusions can easily be extended to more general situations.

199   For the present purpose, the main quantities of interest are the sojourn time densities $t^*(x, q)$

200   and $t^{**}(x, q)$, defined in the Material and Methods, Numerical integrations. These are expressed in

201   units of the coalescent time $2N_e$; the corresponding absolute times can be obtained by multiplying

202   by $2N_e$. When A_2 is initially present as a single copy, only the situation when $q \leq x \leq 1$ need be

203   considered; the relevant expressions for $t^*(x, q)$ and $t^{**}(x, q)$ are given in the Appendix.

204   Approximations obtained by using only first- and second-order terms in γ are given by Equations

205   (A5) and (A7), for $t^*(x, 1/N_H)$ and $t^{**}(x, 1/N_H)$, respectively.

206   Equations (A5) and (A7) can be integrated over the interval $1/N_H \leq x \leq 1$, yielding

207   approximate expected conditional times to fixation and loss for a new mutation. We have:

208

209                    $$t^* \approx 2\{1 - \tfrac{1}{18}\gamma b - \tfrac{1}{18}\gamma^2[a(a + b) + \tfrac{59}{300}b^2]\} \qquad\qquad (2)$$

210

211        $$t^{**} \approx 2N_H^{-1}\{\ln(N_H) - 1 - \tfrac{5}{18}\gamma b - \tfrac{1}{18}\gamma^2[a(5a + \tfrac{7}{2}b) + \tfrac{17}{100}b^2]\} \qquad (3)$$

212

213

214   For greater accuracy, Euler's constant (0.5772..) should be added to the terms inside the brackets

215   on the right-hand side of Equation (3), to correct for the difference between the summation and

216   integration of $1/x$ (Ewens 2004, p.23). Kaushik and Jain (2021, Equation 9) have independently

217   derived an approximation similar to Equation (2) for the case of an autosomal locus and random

218   mating. Their H corresponds to $h - \frac{1}{2}$; if terms in H^2 are neglected, their equation is the same as

219   Equation (2), except for the fact that their expression for t^* differs by a factor of $\frac{1}{2}$, because of their

220   assumption of a continuous time birth-death process rather than a Wright-Fisher model.

221   The first-order terms in γ in these equations show that when $b > 0$ ($h < 0.5$ in the case of

222   autosomal inheritance), the mean times to fixation and loss of a favorable mutation ($\gamma > 0$) are

223   reduced below their neutral value, if γ is sufficiently close to 0. These times are increased when $b <$

224   0 ($h > 0.5$ with autosomal inheritance). The converse relations hold for the case of a deleterious

225   mutation ($\gamma < 0$). These results correspond to those of Mafessoni and Lachmann (2015), based on

226   numerical evaluations of the relevant general equations. Furthermore, when $b = 0$ (corresponding to

227   semi-dominance with diploid inheritance), t^* and t^{**} are at a maximum with respect to γ when $\gamma =$

228   0, so that selection on a semi-dominant autosomal mutation (or a semi-dominant mutation with

229   respect to female fitness, with X-linkage) is always associated with a shorter conditional time to

230   fixation or loss than under neutrality.

231   The quadratic terms in γ in Equations (2) and (3) are positive for biologically realistic values

232   of a and b (see Box 1 of Charlesworth [2020a]), so that sufficiently strong selection causes t^* and

233   t^{**} to decline with γ, as was found numerically by Mafessoni and Lachmann (2015) for the case of

234   autosomal inheritance and random mating. Furthermore, the expressions for a and b in Box 1 of

235   Charlesworth (2020a) show that, if the sign of γ is changed, t^* remains the same if the dominance

236   coefficient h is changed to the complementary value of $1 - h$, generalizing the result of Maruyama

237   and Kimura (1974). This is not true of t^{**}, however. For the case of an autosomal mutation with

238   random mating, the leading term in the multiplicand of $-\gamma^2/18$ in Equation (3) is equal to $h(7 -$

239      $4h)/2$. Substitution of $1 - h$ for h yields a multiplicand with a leading term of $(1 - h)(10 - 3h)/2$, and

240   the difference between the two multiplicands is $[h(20 - 7h) - 10]/2$. If $h \leq 0.5$, this expression is

241   always negative, implying that a weakly selected partially recessive deleterious mutation with

242   dominance coefficient $h < 0.5$ will (somewhat paradoxically) experience a longer mean time to loss

243   than the reverse favorable mutation with dominance coefficient $1 - h$. This is of interest for the

244   main topic of this paper, because the flux of mutations between deleterious and favorable alleles at

245   a site is the basis of the analysis of the long-term effects of weak selection on variability (see the

246   section below on *Relevance to associative overdominance and background selection*).

247   A similar treatment can be given for the means of the sum of the diversity $2x(1 - x)$ in each

248   generation over the paths to fixation or loss of a new mutation (H^* and H^{**}, respectively), which

249   are obtained by integrating the product of $4N_e\, x(1 - x)$ with $t^*(x, q)$ or $t^{**}(x, q)$, respectively, over x

250   between 0 and 1. The relevant integrations give:

251

$$H^* \approx \tfrac{4}{3}N_e\{1 - \tfrac{1}{15}\gamma b - \tfrac{1}{15}\gamma^2[a(a + b) + \tfrac{4}{21}b^2]\} \tag{4}$$

253

$$H^{**} \approx \tfrac{8}{3}N_H^{-1}N_e\{1 - \tfrac{2}{15}\gamma b - \gamma^2[\tfrac{2}{15}a^2 + \tfrac{1}{10}ab + \tfrac{1}{210}b^2]\} \tag{5}$$

255

256   These expressions show that H^* and H^{**} have similar properties to t^* and t^{**} with respect to

257   their dependence on b when selection is sufficiently weak that first-order terms in γ predominate.

258   Weak positive or negative selection with $\gamma b < 0$ can thus result in an increase in these measures of

259   diversity relative to neutral expectation, contrary to what is commonly assumed in discussions of

260   molecular variability. In addition, H^* has the same properties as t^* with respective to the sign of

261   γ and the complementary dominance coefficients h and $1 - h$, which follows from the fact that H^*

262   differs from t^* only by a factor of $4N_e x(1 - x)$ when integrating its product with $t^*(x, q)$ with respect

263   to x.

264   The sojourn time density function in Equation (A7) can be used to find the corresponding

265   net mean sojourn time between loss or fixation for a new mutation, to an accuracy of order γ^2:

266

$$t \approx 2N_H^{-1}\{\ln(N_H) + 0.5772 + \gamma a - \tfrac{1}{36}\gamma^2 b(5a + b)\} \tag{6}$$

268

269   Similarly, the expected sum of the diversity values over the sojourn of a mutation in the

270   population before its loss or fixation is approximated by:

271

$$H \approx 4N_e N_H^{-1}\{1 + \tfrac{1}{3}\gamma a - \tfrac{1}{18}\gamma^2 b(a + \tfrac{1}{5}b)\} \tag{7}$$

273

274   With respect to terms of the first order in γ, there is no dependence on γb of the net mean

275   sojourn time and net diversity, but they are both increasing functions of γa. This is consistent with

276   the classical result for the case of a semi-dominant autosomal mutation with random mating, where

277   H is an increasing function of γ (Fisher 1930, Figure 3; Kimura 1983, p.44). At first sight, it seems

278   paradoxical that semi-dominant mutations subject to positive selection should yield a higher net

279   diversity than neutral mutations during their sojourn in the population. But this is simply a

280   reflection of the fact that they have a higher chance of establishing themselves in the population,

281   and hence of contributing to diversity.

282

283   **Numerical results for times to loss and fixation and net diversity**

284   The accuracy of these approximations was checked by comparison with the results of numerical

285   integrations of the relevant diffusion equation formulae, as described in the Material and Methods

286   and the Appendix, and by computer simulations of an autosomal locus in a randomly mating

287   population of size N, with binomial sampling of post-selection gametes. In this case, $N_e = N$ and N_H

288    $= 2N$. Figure 1 shows the mean fixation times of a new mutation (conditional on its fixation) for a

289   range of values of $|\gamma| = 2N_e |s|$. Both deleterious mutations ($s < 0$) with dominance coefficient $h =$

290   0.1 and favorable mutations with dominance coefficient $h = 0.9$ ($s > 0$) were modeled. The values

291   for a neutral mutation, obtained by integration of the sojourn time density function in the absence of

292   selection with respect to x between $1/N_H$ and $1 - 1/N_H$, are indicated by the horizontal lines. The

293   results from the numerical integrations of the sojourn time densities (black curves) are in close

294   agreement with the simulation results (red points) over the whole range of γ values used here. The

295   approximate values from Equation (2) (blue curves) are in good agreement with the more exact

296   values for $|\gamma|$ up to 2 or so, but then tend to overestimate the fixation times. Nonetheless, the

297   qualitative pattern of an increase in fixation time above the neutral value as $|\gamma|$ increases to a value

298   near 2, followed by a decrease, is captured by the approximation. The more exact results show that

299   the neutral value of t^* is returned to more quickly, at $|\gamma| \approx 3$, than is indicated by the approximation.

300   As expected from the results of Maruyama (1972) and Maruyama and Kimura (1974), the curves

301   for favorable and deleterious mutations, with their complementary values of h, are identical.

302   Figure 2 shows similar results for the mean times to loss of new mutations, conditioned on

303   their loss. These are necessarily much smaller than the mean times to fixation, and are also inverse

304   functions of the population size when measured on the coalescent timescale of $2N_e$ generations, as

305   implied by Equation (3). In terms of generations, the loss times are logarithmically increasing

306   functions of N, since $N_e = N$ in the cases shown here. There are noticeable differences between the

307   results for deleterious and favorable mutations, with the partially deleterious mutations having

308   longer mean times to loss than the complementary partially dominant favorable mutations, due to

309   the multiplicands of $-\gamma^2$ being smaller for the deleterious than the complementary favorable

310   mutations, as noted in the previous section. Similarly, the deleterious mutations return to the neutral

311   value at larger values of $|\gamma|$ than the complementary favorable mutations. The multiplicand of $-\gamma b$

312   is larger for losses than fixations, so that the condition on $|\gamma|$ for t^{**} to exceed the neutral value is

313   more liberal for losses than for fixations. However, the second-order terms in both cases are always

314   positive, and overcomes the first-order terms when $|\gamma|$ is large enough.

315   Similar patterns of behavior are found for the mean sums of the diversities over the course

316   of fixations and losses, H^* and H^{**}; examples similar to those in Figures 1 and 2 are shown in

317   Figures S1 and S2, using the integration and approximate results. As might be expected, H^* and

318    $H^{**}$are closely correlated with t^* and t^{**}, respectively (Figure S3).

319   Figure 3 shows the approximate and integration results for the conditional mean times to

320   fixation and loss for the whole range of dominance coefficients, with $|\gamma| = 1$ or 2. The

321   approximations (solid curves) agree very well with the integration results (dashed curves) for both

322   strengths of selection, and are nearly linear in h. As expected from Equations 2 and 3, the

323   relationships of the fixation and loss times to h for the deleterious and favorable mutations are

324   opposite in direction, with deleterious mutations having fixation and loss times that decrease with h,

325   whereas those for favorable mutations increase with h. Weaker selection is associated with a larger

326   range of h values for which the fixation time is greater than the neutral value.

327   A critical value of the dominance coefficient for a given γ, $h_{cf}(\gamma)$, can be defined, which is

328   the value of h at which the mean fixation time is equal to the neutral value. A similar quantity,

329    $h_{cl}(\gamma)$, can be defined for the mean time to loss. As is discussed in more detail in the section

330   *Relevance to associative overdominance and background selection*, these quantities provide a

331   useful link between the present approach and that of Zhao and Charlesworth (2016), who examined

332   the conditions for AOD versus BGS for the case of a large population that is initially in statistical

333   equilibrium under mutation, drift and selection, and then suffers a permanent reduction in

334   population size. As a measure of the magnitude of genetic drift, they used the asymptotic rate at

335   which variability at a neutral site linked to a site under selection decreases after the reduction in N,

336   and determined whether selection increased or reduced the rate of loss of variability.

337   Approximations for the critical dominance coefficients that correspond to the boundary

338   between an increased and a decreased mean fixation or loss time can be obtained by setting the sum

339   of the terms involving γ and γ^2 to zero in Equations (2) and (3), and solving the resulting quadratic

340   equations in h. For $h_{cf}(\gamma)$, the further approximation of replacing 59/300 with 1/5 is used.

341   After some algebra, the following expressions are obtained:

342

343
$$h_{cf}(\gamma) \approx \tfrac{1}{2}\gamma^{-1}\{\gamma - 10 + 10\sqrt{1 + 0.05\gamma^2}\} \qquad (8a)$$

344
$$h_{cl}(\gamma) \approx (0.264\gamma)^{-1}\{0.282\gamma - 1 + \sqrt{1 - 0.3\gamma + 0.08550\gamma^2}\} \qquad (8b)$$

345

346   As γ approaches zero, consideration of the leading terms in γ in the radicals in these

347   equations shows that the critical dominance coefficient $\approx 0.5 + 0.125\gamma$ in both cases, so that slightly

348   recessive mutations ($\gamma < 0$) or dominant mutations ($\gamma > 0$) result in an increase in mean fixation and

349   loss times when selection is very weak. For small γ, which is the main region of interest as far as

350   AOD is concerned, the critical dominance coefficients are nearly linear in γ (Figure 4).

351   The blue curves in Figure 4 show the critical dominance coefficients for the operation of

352   AOD, given by the solution of the approximate cubic Equation (18) of Zhao and Charlesworth

353   (2016). For favorable mutations, this expression breaks down for $\gamma > 1.26$, but performs well for

354   deleterious mutations over the entire range displayed. If the cubic equation is approximated by

355   ignoring terms in γ^2, the critical dominance coefficient for the operation of AOD is $0.5 + 0.125\gamma$, the

356   same as for h_{cf} and h_{cl}. This suggests that the two approaches are related to each other, although the

357   three different functions describing h_c do not agree precisely.

358

359   **Effects of weak selection on variability at linked neutral sites**

360   Intuitively, one would expect the longer mean fixation times associated with weak selection and γb

361   < 0 to produce a higher level of mean pairwise diversity (π) at a linked neutral site than when a

362   neutral mutation has become fixed. This was shown to be the case by Mafessoni and Lachmann

363   (2015) and Johri *et al.* (2021), using computer simulations (similar, but smaller, effects would be

364   expected from losses of new mutations; these were not, however, examined in these papers). Note,

365   however, that the fixation of a neutral mutation produces an approximately 42% reduction in π at

366   completely linked sites (Tajima 1990), so that all these cases are still associated with reduced rather

367   than increased diversity. This is because π is measured at a single point in time (when a new

368   mutation has been fixed), rather than using an estimate of the mean of π over a long time period at a

369   focal neutral site that is subject to a succession of evolutionary events at a linked site – if this site is

370   neutral, the mean π at the focal site cannot be affected by these events. An approximate method for

371   calculating π at the end of a fixation event was used by Johri *et al.* (2021), based on the selective

372   sweep equations of Charlesworth (2020b); this procedure is, however, unsatisfactory, since the

373   sweep equations are inaccurate at small $|\gamma|$ values.

374   A first step towards obtaining an estimate of the long term mean value of π is to determine

375   the pattern of variability at a focal neutral site over the course of fixation (or loss) of a linked

376   mutation (A_2) introduced into a population initially fixed for the alternative allele (A_1). This was

377   done here by applying the simulation procedure of Tajima (1990), as described in the Material and

378   Methods section and in Johri *et al.* (2021). The left-hand panel in Figure 5 shows the results for

379   fixations of a favorable mutation with dominance coefficient $h = 0.9$ and a range of γ values, in a

380   population size of 50, and with complete linkage between the neutral and selected sites. All

381   diversity statistics are measured relative to $\theta = 4N_e\mu$, the equilibrium value in the absence of

382   selection. It will be seen that the mean relative π over all genotypes taken over a fixation event (π_w)

383   exceeds one for sufficiently small γ values, even for the neutral case of $\gamma = 0$, whereas the relative π

384   at the time of fixation or loss is always < 1. The reason for the excess in π_w over neutral expectation

385   is that the slowness of the fixation process (whose expected value is of the order of $4N_e$ generations

386   with weak selection) allows A_1 and A_2 haplotypes to diverge in sequence over the course of the

387   fixation of A_2, because their mean coalescent times in the absence of recombination are much

388   greater than the standard neutral value of $4N_e$ generations (Kimura and Ohta 1969). Comparable

389   results are seen for losses of new mutations, but with much smaller effects due to the shorter

390   expected duration of loss events, which is close to $2 \ln(N_H)$ generations with weak selection (Figure

391   S4).

392   These results yield the seemingly paradoxical conclusion that fixation and loss events can be

393   associated with a net increase in mean π at linked neutral sites during the course of fixation or loss,

394   even when they involve neutral mutations. The paradox with respect to neutral mutations comes

395   from the fact that one type of conditional event has been replaced by another: we are conditioning

396   on observing a fixation or loss event that is in progress. The following approximate approach avoids

397   such conditioning. As was done by Charlesworth (2020b) for the case of sweeps of strongly

398   selected mutations, ergodicity is assumed: the probability of a given value of π resulting from the

399   hitchhiking effects of the selected site is proportional to the amount of time that the process spends

400   at that value of π, analogous to the use of the sojourn time density for determining the frequency

401   spectrum at a single locus (Ewens 2004 pp.24-25).

402   A core assumption is that the rates of fixation and loss events are sufficiently low that the

403   intervals between successive events allow a complete recovery of diversity. Once again, diversities

404   are measured relative to the value in the absence of selection, and the deviation of the relative

405   diversity value from one is denoted by $\Delta\pi$. If the mean value of $\Delta\pi$ immediately after a given

406   fixation or loss event is denoted by $\Delta\pi_0$, and the value of $\Delta\pi$ at time t after such an event is $\Delta\pi_t$, we

407   have $\Delta\pi_t \approx \Delta\pi_0 \exp(-t)$, where t is in units of $2N_e$ generations (Malécot 1969, p.40; Wiehe and

408   Stephan 1993, Equation 6a). The sum of the values of $\Delta\pi_t$ over subsequent generations, relative to

409     $2N_e$, can thus be approximated by:

410

411
$$\Delta\pi_0 \int_0^\infty \exp(-t) \ \mathrm{d}t = \Delta\pi_0 \qquad\qquad (9)$$

412

413   We also need to consider the contribution from the mean diversity over the course of each

414   fixation (loss) event, which is given by the expectation of the product of the duration of an event,

415   T_e, and the associated mean value per generation of $\Delta\pi$ over the course of the event, $\Delta\pi_w$, *i.e.*, by

416     $\mathrm{E}\{T_e\Delta\pi_w\}$. If T_e is measured in units of coalescent time, the sum of the $\Delta\pi$ values relative to $2N_e$

417   over a long period of time (or over many independent pieces of genome that are all subject to the

418   same evolutionary process) the mean sum of the deviation of the relative diversity from 1 over the

419   between successive fixation (loss) events is given by:

420

421     $$\Delta\pi_S = \Delta\pi_0 + \mathrm{E}\{T_e\Delta\pi_w\} \qquad\qquad (10)$$

422

423   To calculate the change in mean relative diversity due to a succession of evolutionary

424   events, we would of course need to know the total length of time involved, requiring a calculation

425   of the expected number of occurrences of fixation (loss) events and the expected times between

426   them (see the next section). Use of Equation (10) avoids having to make a detailed model of these

427   events, and provides an index of the expected magnitude and sign of the effects on neutral diversity

428   of fixations (losses) at a linked site. $\Delta\pi_S$ can thus be (loosely) referred to as the mean change in

429   diversity associated with a series of fixation or loss events.

430   It should be noted that the assumption of an indefinitely large amount of time for recovery

431   of diversity between fixation or loss events implies that the contribution of $\Delta\pi_0$ relative to $\mathrm{E}\{T_e\Delta\pi_w\}$

432   is overestimated compared with a realistic evolutionary model, so that any increases in diversity

433   with weak selection when $\gamma b < 0$ will be underestimated by this approach when $\Delta\pi_0 < 0$ and

434     $\mathrm{E}\{T_e\Delta\pi_w\} > 0$.

435   Numerical values of the quantities involved can be obtained from the simulations of a

436   neutral sites linked to a locus subject to selection, using the algorithm of Tajima (1990), as

437   described in the Material and Methods. The relevant statistics are shown in the left-hand panel of

438   Figure 5 for the case of the fixation of a partially dominant favorable mutation ($h = 0.9$) in a

439   population with $N = 50$. Using Equation (10), $\Delta\pi_S$ for recurrent fixations is shown in the right-hand

440   panel of Figure 5, for $N = 50$ and $N = 500$. Here, the mean of $T_e\Delta\pi_w$ over many replicate simulations

441   is used as an estimate of $\mathrm{E}\{T_e\Delta\pi_w\}$.

442   It can be seen that fixations of highly dominant, favorable mutations cause an increase in

443   diversity when γ is sufficiently small, but diversity is reduced when γ is somewhat greater than 2;

444   the value of γ at the point of return to a reduction in π is smaller with the larger value of N. As

445   expected from the properties of the mean fixation time described above, a similar pattern (within the

446   limits of statistical error) is observed for fixations of deleterious mutations with $h = 0.1$ and the

447   same absolute value of γ (Figure S4). Figures 6 and S5 show comparable results for losses of both

448   favorable and deleterious mutations; in this case, the patterns are noticeably different for the two

449   types of mutations, and are much more strongly affected by the population size, as expected from

450   the corresponding effects on mean loss times described in the previous section. Tables S1-S8 show

451   the detailed statistics for the simulations on which these figures are based, and Table S9 shows

452   summary diversity statistics for fixation and loss events for a range of dominance coefficients, and

453   two different strengths of positive and negative selection.

454   The results described here allow questions to be asked about the nature of the major

455   determinant of the effect of selection on neutral diversity at a linked site. Intuitively, it would seem

456   likely that the mean conditional sojourn times t^* and t^{**} must play a major role, and that the answer

457   depends on what aspect of diversity is being explored. The results shown in Table S9 can be used to

458   assess the relations between various diversity statistics and the sojourn times for a range of h values

459   and two different $|\gamma|$ values, displayed in Figures S6-S11. Here, the results for $\gamma > 0$ and $\gamma < 0$ are

460   shown in the same panels. For fixations, Figures S6-S8 show that $\Delta\pi_S$, $\Delta\pi_w$ and $-\Delta\pi_0$ are all nearly

461   linearly related to t^* for a given $|\gamma|$ value, with $\Delta\pi_S$ and $\Delta\pi_w$ increasing with t^* and $-\Delta\pi_0$ decreasing

462   with t^*. The plots for $\Delta\pi_S$ and $\Delta\pi_w$ are displaced downwards for the larger $|\gamma|$ value, whereas the

463   plot for $-\Delta\pi_{0f}$ is displaced upwards. The reduction in diversity at the end of a fixation event $(-\Delta\pi_0)$

464   is generally somewhat smaller for a given value of t^* for $\gamma < 0$ than for $\gamma > 0$, but a nearly linear

465   relationship with t^* holds for a given value of γ.

466   As might be expected from the fact that t^{**} is different for mutations with a given $\gamma > 0$ and

467     $\gamma < 0$ and dominance coefficients of h and $1 - h$, respectively, the pattern is more complex for loss

468   events. The plots for $\Delta\pi_S$ and $\Delta\pi_w$ fall into two branches, with the left-hand branch for $\Delta\pi_S$

469   corresponding to $\gamma < 0$ and the right-hand branch $\gamma > 0$, and vice-versa for $\Delta\pi_w$. Within branches, the

470   relations of $\Delta\pi_S$ and $\Delta\pi_w$ to t^{**} are similar to those for fixation events. Interestingly, the relation of

471   t^{**} to $-\Delta\pi_0$ is in the opposite direction to that between of t^{**} to $-\Delta\pi_0$. For the stronger selection

472   intensity, no division into two branches is seen for $-\Delta\pi_0$; for the weaker selection case, there is a

473   very clear division, with the lower set corresponding to $\gamma < 0$.

474   These results show that, for a given value of γ, the sojourn times are nearly linearly related

475   to the diversity statistics, but both the sign and magnitude of γ influence the values of the diversity

476   statistics for the same value of t^* or t^{**}. There is a close correspondence between the values of t^*

477   and t^{**} that are generated by the simulations with $\gamma = 0$ and the thresholds at which $\Delta\pi_S \geq 0$, within

478   the limits of sampling error (Figures S6 and S9); the simulation values have been used rather than

479   the integrations, as the latter are slightly inaccurate for $N = 50$ (Figures 1 and 2).

480   Another complexity is revealed by the comparison of the results on fixation with $h = 0.9$ and

481    $h = 0.1$ for a given value of $|\gamma|$ (Tables S6-S8). Especially for the larger values of $|\gamma|$, $\Delta\pi_S$ is larger

482   for deleterious mutations with $h = 0.1$ than for favorable mutations with $h = 0.9$ and the same $|\gamma|$,

483   even though t^* is the same in both case. For example, $\Delta\pi_S = 0.0384\pm0.0036$ for $\gamma = -2$ and $h = 0.1$,

484   but $\Delta\pi_S = 0.0325\pm0.0035$ for $\gamma = 2$ and $h = 0.9$; for $|\gamma| = 5$, the corresponding values of $\Delta\pi_S$ are $-$

485   0.200 ± 0.003 and -0.228 ± 0.002, a nearly 30% difference.

486   This sheds some light on the causes of the relation of $\Delta\pi_S$ to t^*. As the duration of a fixation

487   event increases, the mean neutral diversity of haplotypes carrying the selectively favorable A_2

488   variant increases, because these haplotypes spend longer in the population before reaching fixation

489   and hence have a longer coalescence time. The divergence between A_1 and A_2 haplotypes also

490   increases with t^*, since a longer time is available for them to diverge. The changes in the diversity

491   of A_1 haplotypes are more minor. The net result is that the net mean diversity over the course of the

492   event ($\Delta\pi_w$) increases with t^*, as can be seen in Figure S7, so that its product with t^*, which appears

493   in the equation for $\Delta\pi_S$ (Equation 10) also increases with t^*. This effect is reinforced by the decline

494   in the reduction of diversity at the time of fixation of A_2, $-\Delta\pi_0$, as t^* increases (Figure S8),

495   reflecting a greater coalescence time for A_2 when its sojourn time is longer.

496   These considerations apply to both positive and negative selection. However, with positive

497   selection, A_2 spends more of its time at high frequencies than at low frequencies before becoming

498   fixed, whereas the reverse is true with negative selection, as can be seen in the plots of the sojourn

499   time densities relative to the neutral values that are shown in Figure 8 (note that $t^*(x)$ is independent

500   of x in the absence of selection). This means that, for the same $|\gamma|$ value, haplotypes carrying A_1

501   have a longer coalescence time with negative than with positive selection; because these haplotypes

502   start with the equilibrium neutral diversity value θ, they contribute disproportionately to $\Delta\pi_w$. This

503   effect is especially clear for the larger values of $|\gamma|$; for example, with $|\gamma| = 5$, the mean diversity of

504   A_1 haplotypes is 0.657 ± 0.001 for $\gamma = -5$, and 0.608 ± 0.001 for $\gamma = 5$.

505   A similar pattern is seen with losses of mutations. This is perhaps less surprising, since t^{**}

506   for a given $|\gamma|$ value is greater for deleterious mutations than for favorable mutations with the

507   complementary dominance coefficient (Figure 3). However, Tables S5-S8 show that the diversity of

508   A$_1$ haplotypes is smaller for negative selection than for positive selection with the complementary

509   dominance coefficient; it decreases with t^{**} with negative selection and increases with positive

510   selection. This reflects the fact that a longer duration of the time to loss implies a smaller overall

511   population size for A$_1$. This also explains the fact that the final diversity reduction increases with

512   t^{**} – this reduction is measured at the time A$_1$ becomes fixed, and hence reflects the history of

513   population size change for A$_1$ haplotypes.

514

515   **Relevance to associative overdominance and background selection**

516   As mentioned in the Introduction, the relevance of these results to associative overdominance

517   (AOD) arises from the fact that, if selection is sufficiently weak in relation to genetic drift, a

518   biallelic locus subject to selection and reversible mutations will experience a constant flux of

519   mutations from the states of fixation for A$_1$ to fixation for A$_2$ and vice-versa, as in the Li-Bulmer

520   model of codon usage bias (Li 1987; Bulmer 1991; McVean and Charlesworth 1999). Here, A$_1$ is

521   now used to denote the selectively favorable allele at a given site, and A$_2$ its deleterious alternative,

522   rather than ancestral and mutant alleles, respectively. For the case of an autosomal locus, the

523   relative fitnesses of the three genotypes A$_1$A$_1$, A$_1$A$_2$ and A$_2$A$_2$ are 1, $1 - hs$ and $1 - s$, respectively (s

524   ≥ 0); with weak selection, this is equivalent to representing these fitnesses as $1 + s$, $1 + (1 - h)s$ and

525   1. Thus, if the deleterious effects of A$_2$ are recessive or partially recessive ($0 \leq h < 0.5$) and $\gamma = 2N_e s$

526   is sufficiently small, the entry of an A$_2$ mutation into a population temporarily fixed for A$_1$ will be

527   associated with a longer net sojourn time in the population than that for a neutral mutation. The

528   same applies to the entry of a favorable A$_1$ mutation into a population temporarily fixed for A$_2$.

529   The results in the previous section strongly suggest that, under these conditions, diversity at

530   closely linked neutral sites will be enhanced when a stationary state with respect to mutation,

531   selection and drift is reached. The effect of the constant flux of mutations at a selected site on the

532   expected level of neutral diversity (π) at the linked neutral site can be determined with the use of the

533   ergodic assumption. This allows the application of the results of the simulations described above

534   that used this approach, employing the infinite sites assumption that mutations are sufficiently

535   infrequent that new mutations occur only at sites that are fixed for either A$_1$ or A$_2$, which was

536   applied to the theory of codon usage by Bulmer (1991) and McVean and Charlesworth (1999).

537   Table 1 shows the variables that are used in this procedure. As in the previous section, diversity is

538   measured relative to the purely neutral equilibrium value $\theta = 4N_e \mu$, and its deviation from one at

539   given point in time is denoted by $\Delta\pi$.

540   Consider a site that has just become fixed for A_1. Under the above assumptions, the

541   distribution of times until an A_2 mutation arises and becomes fixed is exponential, with parameter

542   λ_{11}. If a time t is drawn from this distribution, the expected number of A_2 mutations that arise and

543   become lost during an interval of length t is $\lambda_{10} t$, where $\lambda_{10} \gg \lambda_{11}$ from the formulae in Table 1.

544   Integrating over the distribution of t, the expected number of losses of A_2 mutations before A_2

545   becomes fixed is found to be approximately equal to $\lambda_{10} / \lambda_{11} = P_{10}/P_{11}$. If the times between each

546   successive event are $\gg 1$, diversity completely recovers between loss events, and between the

547   initial fixation and first loss event (it is shown below that this assumption can be relaxed). Applying

548   Equation (10) from the previous section, and using the notation in Table 1, the expected sum

549   (relative to $2N_e$) of $\Delta\pi$ values at the neutral site over the interval between the successive fixation

550   events A_2 to A_1 and A_1 to A_2 is given by:

551

552     $$\Delta\pi_1 \approx \Delta\pi_{1f} + (\lambda_{10} / \lambda_{11}) \, \Delta\pi_{10S} \qquad\qquad (11a)$$

553

554   A similar argument applies to the interval succeeding the fixation of the A_2 mutation and

555   another fixation of an A_1 mutation, substituting 2 for 1 in the first subscripts for the Ps and λs in

556   Table 1 ($\lambda_{20} \gg \lambda_{21}$ is assumed), giving:

557

558     $$\Delta\pi_2 \approx \Delta\pi_{2f} + (\lambda_{20} / \lambda_{21}) \, \Delta\pi_{20S} \qquad\qquad (11b)$$

559

560   The expectation of the sum of $\Delta\pi$ values over an entire cycle between successive fixations

561   of A_1 mutations is simply $\Delta\pi_T = \Delta\pi_1 + \Delta\pi_2$. We can thus estimate the expected value of $\Delta\pi_T$ per

562   generation, $\Delta\pi_e$, by dividing $\Delta\pi_T$ by the expected time between successive fixations of A_1 (in units

563   of $2N_e$ generations), $T_s = (\lambda_{11}^{-1} + \lambda_{21}^{-1})$:

564

565     $$\Delta\pi_e = \frac{\Delta\pi_1 + \Delta\pi_2}{T_s} \qquad\qquad (11c)$$

566

567   It is useful to note that the expression for T_s is consistent with the existence of a stationary

568   state for the proportion of sites fixed for A_1 versus A_2, using the infinite sites assumption. If these

569   proportions are denoted by X and $1 - X$, respectively, stationarity exists if $\lambda_{11}X = \lambda_{21}(1 - X)$, i.e., $X =$

570     $\lambda_{21}/(\lambda_{11} + \lambda_{21})$ (Bulmer 1991; McVean and Charlesworth 1999). At stationarity, the proportion of

571 sites that are fixed for A_1 is proportional to the expected time a site spend in that state, so that $X =$

572 $\lambda_{11}^{-1}/(\lambda_{11}^{-1} + \lambda_{21}^{-1}) = \lambda_{21}/(\lambda_{11} + \lambda_{21})$.

573   All the quantities needed for determining the value of $\Delta\pi_e$ in Equation (11c), other than the

574 mutational parameters at the selected site, θ_s and κ, can be obtained from the integral formulae for

575 the fixation probabilities, together with the simulation methods described in the previous section.

576 The mutational parameters serve only to determine the magnitude of $\Delta\pi_e$, and have no influence on

577 its sign, provided that the assumptions concerning the times to recovery after fixation and loss

578 events and the relative values of λ_{i0} and λ_{i1} are met. The general equations above are valid regardless

579 of the frequency of recombination; the values of the $\Delta\pi$ variables that appear in these expressions

580 will, of course, be affected by recombination.

581   Figure 7 shows an example of estimates of $\Delta\pi_e$ for the case of a neutral locus that is

582 completely linked to a selected locus with equal mutation rates in each direction between

583 deleterious and favorable alleles ($\kappa = 1$), as a function of the scaled selection coefficient, γ. The

584 deleterious allele (A_2) has dominance coefficient $h = 0.1$, such that the relative fitnesses of

585 heterozygotes and homozygotes for this allele are $1 - 0.1s$ and $1 - s$, respectively. As expected from

586 the previous results, the enhancement of diversity is maximal (approximately 0.008 with $N = 500$)

587 when $\gamma = 1.5$. The fact that $\Delta\pi_e$ is significantly negative for $\gamma = 0$ suggests that, as noted above, the

588 assumption of a long recovery period between successive losses or fixations at the selected locus

589 results in an underestimation of $\Delta\pi_e$ for small γ. In the example in the figure, the scaled mutation

590 rate at the selected locus was 0.01 for both population sizes, corresponding to an absolute mutation

591 rate of 5×10^{-5} with $N = 50$ and 5×10^{-6} with $N = 500$; the results are not very sensitive to the

592 absolute value of N for the same set of scaled parameters, so that the approximate values for an

593 arbitrary θ_s can be obtained by multiplying the results in the figure by $100\theta_s$. In a population of size

594 10,000, the mutation rate would be 1.25×10^{-7}, corresponding to a non-recombining region with 25

595 basepairs under selection, if the mutation rate is 0.5×10^{-8} per basepair, which is approximately the

596 same as the estimate for *Drosophila melanogaster* (Assaf *et al.* 2017).

597   A check on the validity of this approach is provided by the case when γ is so large that the

598 rate of fixation of deleterious mutations is negligible. This means that only the state when the

599 population is fixed for the favorable allele A_1 needs to be considered. There is then a constant input

600 of new mutations to A_2 alleles, which are successively lost from the population with a probability

601 close to 1. This situation corresponds to the standard model of background selection (BGS), under

602 which stochastic effects at the loci under selection are assumed to be negligible (Charlesworth et al.

603 1993). In this case, however, the assumption of a complete recovery of diversity at the neutral locus

604   after each loss event is likely to be violated, as the large population size means that there is a high

605   rate of input of new deleterious mutations that are then rapidly lost from the population, especially

606   if we are dealing with a non-recombining region with numerous genes subject to purifying

607   selection.

608   This problem is examined in the second part of the Appendix, where it is shown that the

609   results obtained with the assumption of complete recovery should still provide a good

610   approximation in this case. The deviation of mean relative diversity from one can be predicted from

611   the sum of the $\Delta\pi$ values over the period covering the loss of an A_2 allele and the appearance of a

612   new mutation to A_2, as given by Equation (10), divided by the expected time between successive

613   losses of deleterious mutations (equivalent to multiplication by λ_{10}), as can be seen from Equation

614   (A12). This prediction can be compared to the standard BGS formula for autosomal loci in a

615   randomly mating population, which assumes that allele frequencies subject to selection are

616   unaffected by drift, i.e., $\gamma \gg 1$. In this case, the reduction in diversity relative to neutral expectation

617   at a neutral site completely linked to a selected locus or group of loci is approximately equal to u/hs

618   provided that $u/hs \ll 1$, where u is the net rate of mutation to deleterious alleles (Charlesworth *et*

619   *al.* 1993). This can be equated to $\Delta\pi_e$ for the same values of u, h and s when applying Equation

620   (11c) to the simulations used here. To model large γ values while retaining the assumption of small

621   s, it is necessary to use simulations with a large population size ($N = 500$). To generate these

622   numbers, the scaled rate of mutation to deleterious mutations, θ_s, was arbitrarily set to 1; the values

623   for an arbitrary deleterious mutation rate of u can be found by multiplying these values by $4Nu$.

624   Some examples are shown in Table 2; it can be seen that the predictions from the present approach

625   converge on the values from the large population size formula as $h\gamma$ increases.

626   Stochastic fluctuations in the frequencies of alleles at selected loci are known to reduce the

627   effect of BGS on diversity (Charlesworth *et al.* 1993). Table 1 of Charlesworth *et al.* (1993) gives

628   simulation results for a range of γ values for the case of a non-recombining region with a deleterious

629   mutation rate of $u = 0.005$, $s = 0.1$ and $h = 0.2$, giving $u/hs = 0.25$ The ratio of the negative of the

630   natural logarithm of a simulated value of π/θ to 0.25 provides a measure of the extent of the

631   deviation from the deterministic prediction. These measures (with their standard errors) were as

632   follows: 0.696 ± 0.024 ($\gamma = 20$), 0.892 ± 0.035 ($\gamma = 40$), 0.828 ± 0.054 ($\gamma = 80$) and 1.056 ± 0.049

633   ($\gamma = 180$). The corresponding ratios from the present method for these parameter sets were

634   0.510 ± 0.015, 0.858 ± 0.020, 0.992 ± 0.020 and 1.124 ± 0.016, respectively. In view of the

635   approximations needed to obtain these results, there is reasonably good agreement with the exact

636   simulation results.

637   The argument concerning the effect of the times between events presented in the Appendix

638 can be extended to the case when there is a continual flux between A_1 and A_2 alleles, as in the case

639 of the model of AOD discussed above. Here, the probabilities of fixation of both variants are of the

640 order of $1/N_H$, whereas the probabilities of loss are of the order of one. The expected numbers of

641 loss events between successive fixations are thus of order N_H for both types of event. Provided that

642 N_H is not too small, the argument leading to Equation (A.12) implies that the net effect on diversity

643 is similar to the value when there is a complete recovery between loss events, so that Equation (11c)

644 should provide a good approximation to the effects of successive losses, but there will still be an

645 inaccuracy associated with the recovery period following a fixation event.

646

Discussion

648

649 The analytical and simulation results described here shed light on the effects of the fixations and

650 losses of weakly selected mutations on levels of genetic diversity at linked neutral sites. As

651 described in the previous two sections, these effects can largely be understood in terms of the

652 effects of the selection parameters on the times to fixation or loss, with some slight complications.

653

Fixation and loss times with weak selection

655 One might expect selection on favorable mutations to reduce their mean time to fixation relative to

656 neutrality, and selection against deleterious mutations to have the opposite effect, with the converse

657 applying to losses of mutations. As described above, this is not necessarily the case. Mafessoni and

658 Lachmann (2015) used numerical integration of the relevant diffusion equation formulae for

659 autosomal mutations with random mating to show that the mean fixation times of weakly selected

660 dominant or partially dominant ($h > \frac{1}{2}$) mutations, as well as of weakly selected, recessive or

661 partially recessive ($h < \frac{1}{2}$) deleterious mutations, can be larger than the corresponding neutral

662 values. They also showed that, under similar conditions, the mean times to loss of new mutations

663 are larger than the neutral values. For sufficiently large values of $|\gamma| = 2N_e|s|$, however, fixation and

664 loss times are always lower than the neutral values when there is directional selection ($0 \leq h \leq 1$).

665 The approximations derived here (Equations 2 and 3), which are accurate with respect to second-

666 order terms in γ, confirm these findings (see also Kaushik and Jain 2021, Equation 9). They provide

667 a reasonably good fit to the numerical integration and simulation results for $|\gamma|$ values of the order of

668 2 or less, provided that the population size is sufficiently large (Figures 1 and 2).

669

670   **Effects of weak selection on neutral diversity at linked sites**

671   Mafessoni and Lachmann (2015) also showed that fixations of partially recessive favorable or

672   partially dominant deleterious mutations can increase the mean level of diversity at a linked neutral

673   site, compared with the corresponding values for fixations of neutral mutations, if this is measured

674   at the time of fixation. The conditions for such an increase are similar to those for increased times to

675   fixation (see also Johri *et al.* [2021] and Kaushik and Jain [2021]). The simulation results described

676   here confirm this finding, and give similar results for losses of deleterious mutations (Figures 5, S4

677   and S5). However, the diversity levels at the times of fixation or loss are always lower than the

678   mean equilibrium neutral diversity $\theta = 4N_e\mu$, even if these events involve purely neutral mutations,

679   as was first described by Tajima (1990). As was explained in the section *Effects of weak selection*

680   *on variability at linked neutral sites*, this effect is a consequence of conditioning on an unusually

681   short coalescent time at the neutral site linked to the site under observation, and would not be

682   expected to occur if we observe the mean diversity at this site over a long time period that includes

683   multiple fixation or loss events. The question of whether diversity can be increased above θ by

684   weak selection under appropriate conditions is thus not fully answered by these results.

685   A simple approximate method for evaluating the effects of successive fixations or losses at a

686   site linked to focal neutral site is described above (Equation 10). This combines the sum of the

687   diversities at the focal site over the generations while a fixation or loss event is in progress with the

688   sum of the diversities over the generations that intervene until the next such event, during which

689   diversity recovers towards the neutral equilibrium value. As shown in Figures 5, S4 and S5, the

690   mean diversity taken over all generations during a fixation or loss event can be increased over the

691   neutral value when |γ| is sufficiently small, and $h < \frac{1}{2}$ for deleterious mutations or $> \frac{1}{2}$ for favorable

692   ones, partly due to mutational divergence between the haplotypes carrying the two different alleles

693   at the site under selection. Under suitable conditions (a sufficiently long duration of the fixation or

694   loss event), this effect can outweigh the reduction in diversity at the end of the fixation or loss

695   event, resulting in a net increase in mean neutral diversity when taken over the entire period.

696   These considerations yield the seemingly paradoxical result that neutral diversity can be

697   enhanced by fixations or losses of weakly selected favorable or deleterious mutations, in contrast to

698   the usual assumption that diversity is reduced by fixations of favorable mutations (selective sweeps)

699   or losses of deleterious mutations (background selection). It has, however, long been known that

700   neutral diversity can in principle be increased by selection against deleterious recessive or partially

701   recessive mutations at closely linked sites – the process of associative overdominance or AOD

702   (Frydenberg 1963; Ohta 1971; Latter 1998; Pamilo and Palsson 1998; Palsson and Pamilo 1999;

703   Wang and Hill 1999). A correct analytical treatment of this process has, however, only recently

704   been provided (Zhao and Charlesworth 2016). As shown in Figure 4, the critical dominance

705   coefficient for the operation of AOD versus background selection (BGS) as a function of $|\gamma|$ has

706   similar, but not identical, properties to the conditions for increases over the neutral value of the

707   mean fixation and loss times of new deleterious or favorable mutations.

708   The section *Relevance to associative overdominance and background selection* describes

709   how to relate the simulation results for the effects of selection on the diversity statistics at a linked

710   neutral locus, when there is a continual flux of mutations between sites fixed for deleterious and

711   favorable mutations. Under this scenario, the net mean deviation from one of the ratio of diversity

712   to θ is given by $\Delta\pi_e$ in Equation (11c). Fixations and losses contribute approximately equal amounts

713   to $\Delta\pi_e$; although the effects on diversity of losses are much smaller than those of fixations, this is

714   compensated for by the much higher frequencies of loss events.

715   The results described here provide a new perspective on the relation between AOD and

716   BGS. If one imagines a locus subject to reversible mutation between a wild-type allele (A_1) and a

717   deleterious allele (A_2), the standard model of BGS corresponds to the situation when selection

718   against A_2 is so strong ($|\gamma| >> 1$) that there is effectively no possibility of fixations of reverse

719   mutations to A_1, and the system can be treated as though it is at equilibrium under mutation and

720   selection, as in the standard formulae used to describe the effect of BGS on neutral

721   diversity(Charlesworth, et al. 1993; Hudson and Kaplan 1995; Nordborg, et al. 1996). In reality the

722   population size is finite, so mutations from A_1 to A_2 are constantly occurring and being quickly lost

723   from the population, with a probability close to one when $|\gamma| >> 1$. As shown in Table 2, the

724   application of the approach described here to this situation closely approximates the properties of

725   BGS when finite population size is modeled by exact simulations.

726   If $|\gamma|$ is sufficiently small, however, the effects of genetic drift, reversible mutation between

727   A_1 and A_2 need to be considered jointly, as in the Li-Bulmer model of selection on codon usage (Li

728   1987; Bulmer 1991; McVean and Charlesworth 1999). With $|\gamma| \le 2$ or lso, and the dominance

729   coefficient h for deleterious mutations less than ½, the results enshrined in Equations (11) show that

730   diversity at linked neutral sites can be increased over neutral expectation when the population is at

731   statistical equilibrium under drift, mutation and selection for sites under selection. These findings

732   complement the results of the analysis of AOD by Zhao and Charlesworth (2016), who examined

733   the rate of loss of neutral variability in a population that was initially at statistical equilibrium, and

734   then placed into an environment with a relatively small N_e. As noted already, the conditions on the

735   dominance coefficient as a function of $|\gamma|$ that allow an enhancement of variability are similar for

736   the two approaches. The framework described here is more appropriate than that of Zhao and

737   Charlesworth (2016) for populations maintained for a long time at low effective population sizes, as

738   is the case in some laboratory experiments that have yielded evidence for AOD (Latter 1998), and

739   for low recombining genomic regions in large populations, where recent work has also suggested

740   the operation of AOD (Becher *et al.* 2020; Gilbert *et al.* 2020).

741

742   **Interpreting the effects of selection on t^* and t^{**}**

743   It is of interest to see whether intuitive interpretations can be made of the conditions for increases in

744   for the mean times to fixation (t^*) and loss (t^{**}) over their neutral expectations. One important

745   point to note is that Equations (2) and (3) show that the first-order terms in γa in the expressions for

746   t^* and t^{**} are zero when $b = 0$ ($h = \frac{1}{2}$ for autosomal mutations), so that the conditional sojourn

747   times are then approximately the same as with neutrality when selection is very weak. This finding

748   suggests that the first-order effects of selection that depend on the term in γa in Equation (1) are

749   absorbed into the probabilities of fixation and loss, so that the conditional sojourn times are

750   controlled by γb alone when selection is very weak. Another relevant point is that the relative

751   effectiveness of selection versus drift can be quantified by dividing Equation (1) by $x(1 - x)$, which

752   gives the ratio of the selective change in allele frequency per generation to the sampling variance

753   under drift, $x(1 - x)/2N_e$. This ratio is denoted here by $f(x) = \gamma (a + bx)$. If $\gamma b < 0$, the relative

754   effectiveness of selection in causing a movement of x away from zero, as measured by $f(x)$, is

755   reduced, compared with the quasi-neutral case with $\gamma b = 0$, and decreases as x increases.

756   The condition for weak selection to cause an increase in t^* over neutrality is then relatively

757   easy to interpret (see Mafessoni and Lachmann (2015) for a different viewpoint). If $\gamma > 0$ and $b < 0$

758   ($h > \frac{1}{2}$ for an autosomal mutation), x tends to be decreased by selection compared with quasi-

759   neutrality, especially at larger values of x, so that the net time to reach fixation is increased by

760   selection, and the times spent at larger values of x are increased relative to the neutral case. If $\gamma < 0$

761   and $b > 0$ ($h < \frac{1}{2}$ for an autosomal mutation), there is a stronger tendency for x to move towards

762   zero than under quasi-neutrality; because we are conditioning on fixation of A_2, this causes the

763   sojourn time to be increased over neutrality. The pull towards lower values of x is weaker for small

764   x, so that the time spent at low values of x is increased relative to the neutral case. These effects on

765   the sojourn time densities at different frequencies are illustrated in the lower panels of Figure 8.

766   It is less easy to interpret the properties of t^{**}, because the argument used for t^* would at

767   first sight suggest a reduction rather than an increase in t^{**} when $\gamma b < 0$. The most plausible

768   interpretation is that losses of new mutations are largely caused by drift, and take place rapidly as

769   long as x remains close to zero. However, the time for an A_2 mutation to reach a relatively high

770   frequency is increased by weak selection when $\gamma b < 0$. It is then relatively immune to loss, and

771   hence spends longer segregating in the population. This interpretation is consistent with the fact that

772   the sojourn time densities relative to the neutral values are increasing functions of x for both

773   favorable and deleterious mutations, as is shown in the upper panels of Figure 8.

774   A more rigorous way of approaching this question is to use conditional diffusion equations,

775   which depend on the mean change in x for a given x (in units of $2N_e$ generations) for a trajectory

776   conditioned on either fixation or loss (Ewens 2004, p.147; Zhao *et al.* 2015). Denoting the

777   conditional mean changes in x for fixation and loss events by Δx^* and Δx^{**}, respectively, and using

778   primes to denote derivatives, we have:

779

780    $$\Delta x^* = \Delta x + x(1-x)P_1'(x)P_1^{-1}(x) \qquad (12a)$$

781

782    $$\Delta x^{**} = \Delta x + x(1-x)P_0'(x)P_0^{-1}(x) \qquad (12b)$$

783

784   Using Equations (1), (A1) and (A2), these expressions can be approximated as follows, to an

785   accuracy of first-order terms in γ:

786

787    $$\Delta x^* \approx (1-x)(1+\tfrac{1}{3}\gamma bx^2) \qquad (13a)$$

788

789    $$-\Delta x^{**} \approx x\{1+\tfrac{1}{3}\gamma b[1-x(2-x)]\} \qquad (13b)$$

790

791   Consistent with the argument used above, there is no contribution from γa to these

792   expressions. The terms added to Δx in these equations have been called "fictitious selection"

793   by Zhao *et al.* (2025); here, these terms cancel the contribution from γa to Δx. In both cases,

794   the multiplicand of the term in γb is positive for $0 < x < 1$, so that the tendencies for A_2 to

795   increase in frequency relative to the neutral case, as measured by $\Delta x^*/(1-x)$, or to decrease in

796   frequency, as measured by $-\Delta x^{**}/x$, are both reduced when $\gamma b < 0$, implying that the

797   respective sojourn times are increased by selection.

798

799   **Conclusions and future prospects**

800   The work described here illuminate the conditions under which weak directional selection

801   can interact with genetic drift to cause an increase rather than a decrease in genetic diversity

802 at linked neutral sites. It also sheds light on the conditions under which associative

803 overdominance rather than background selection operates. The results are, however, limited

804 in several important respects. First, only the pairwise diversity measure π has been studied, so

805 that the properties of the site frequency spectra at neutral sites linked to the target of selection

806 have not been examined; the results of Mafessoni and Lachmann (2015) and Johri *et al.*

807 (2021) suggest that an increase in variability at a neutral locus caused by fixations of linked

808 weakly selected mutations is accompanied by a reduction in the frequencies of rare variants

809 relative to the standard neutral expectation. Further work is needed to investigate the

810 magnitude of this effect in the context of recurrent fixations and losses of weakly selected

811 mutations, which can cause associative overdominance.

812   Second, the extent to which multiple weakly selected loci will mutually affect each

813 other has largely been unexplored; a recent review of relevant data suggests that such effects

814 of multiple loci may be important for explaining the unexpectedly high levels of inbreeding

815 depression and variation in quantitative traits in small populations (Waller 2021). Previous

816 simulation work has shown that, under the extreme condition of no recombination and many

817 tightly linked highly recessive or deleterious mutations, the population can "crystallize" into

818 two haplotypes carrying complementary sets of mutations that exhibit pseudo-overdominance

819 (Charlesworth and Charlesworth 1997; Palsson 2000); there is evidence for less severe

820 effects, causing a retardation of loss of variability, when multiple loci are subject to

821 deleterious mutations in small populations (Latter 1998; Bersabé *et al.* 2016). Further

822 investigation of this topic is desirable. It would also be of interest to investigate the properties

823 of subdivided populations, where stochastic effects on loci under selection can be significant

824 when deme sizes are sufficiently small (Roze and Rousset 2004; Roze 2015; Charlesworth

825 2018).

826   Finally, the properties of fixation times in varying environments can be significantly

827 different from those for a constant environment that are used here, with a breakdown in the

828 symmetry between h and $1 - h$ for favorable and deleterious mutations as far as t^* is

829 concerned (Kaushik and Jain 2021). It is likely that this will also apply to times to loss. The

830 relations of these quantities with associative overdominance in small laboratory populations

831 will probably not be affected by this effect, but the behavior of natural populations could be

832 significantly changed.

833

834 **Data Availability**

835 No new data or reagents were generated by this research. The codes for the computer programs

836 used to produce the results described below will be made available on Figshare on acceptance.

837

838 **Acknowledgments**

842

843 **Literature Cited**

844 Assaf ZJ, Tilk S, Park J, Siegal ML, Petrov DA. 2017. Deep sequencing of natural and

845   experimental populations of *Drosophila melanogaster* reveals biases in the spectrum of new

846   mutations. Genome Res. 27:1988-2000.

847 Becher H, Jackson BC, Charlesworth B. 2020. Patterns of genetic variability in genomic

848   regions with low rates of recombination. Curr. Biol. 30:94-100.

849 Bersabé D, Caballero A, Pérez-Figueroa A, García-Dorado A. 2016. On the consequences of purging

850   and linkage on fitness and genetic diversity. G3 6:171-181.

851 Bulmer MG. 1991. The selection-mutation-drift theory of synonymous codon usage. Genetics

852   129:897-907.

853 Campos JL, Charlesworth B. 2019. The effects on neutral variability of recurrent

854   selective sweeps and background selection. Genetics 212:287-303.

855 Charlesworth B. 2018. Mutational load, inbreeding depression and heterosis in subdivided

856   populations. Mol. Ecol. 24:4991-5003.

857 Charlesworth B. 2020a. How long does it take to fix a favorable mutation,

858   and why should we care? Am. Nat. 195:753-771.

859 Charlesworth B. 2020b. How good are predictions of the effects of selective sweeps on

860   levels of neutral diversity? Genetics 216:1217-1239.

861 Charlesworth B, Charlesworth D. 1997. Rapid fixation of deleterious alleles by Muller's ratchet.

862   Genet. Res. 70:63-73.

863 Charlesworth B, Jensen JD. 2021. Effects of selection at linked sites on patterns of genetic

864   variability. Ann. Rev. Ecol. Evol. Syst. 52:177-197.

865 Charlesworth B, Morgan MT, Charlesworth D. 1993. The effect of deleterious mutations on

866   neutral molecular variation. Genetics 134:1289-1303.

867 Cutter AD, Payseur BA. 2013. Genomic signatures of selection at linked sites: unifying the

868   disparity among species. Nature Rev. Genet. 14:262-272.

869   Ewens WJ. 2004. Mathematical Population Genetics. 1. Theoretical Introduction. New York:
870   Springer.

871   Fisher RA. 1930. The distribution of gene ratios for rare mutations. Proceedings of the Royal
872   Society of Edinburgh 50:205-220.

873   Frydenberg O. 1963. Population studies of a lethal mutant in *Drosophila melanogaster.* I.
874   Behaviour in populations with discrete generations. Hereditas 50:89-116.

875   Gilbert KJ, Pouyet F, Escoffier L, Peischel S. 2020. Transition from background selection to
876   associative overdominance promotes diversity in regions of low recombination. Curr.
877   Biol. 30:101-107.

878   Hudson RR, Kaplan NL. 1995. Deleterious background selection with recombination.
879   Genetics 141:1605-1617.

880   Johri P, Charlesworth B, Howell EK, Lynch M, Jensen JD. 2021. Revisiting the notion of
881   deleterious sweeps. Genetics 219: iyab094.

882   Kaushik S, Jain K. 2021. Time to fixation in changing environments. Genetics 219: iyab148.

883   Kimura M. 1983. The Neutral Theory of Molecular Evolution. Cambridge: Cambridge
884   University Press.

885   Kimura M. 1971. Theoretical foundations of population genetics at the molecular level.
886   Theor. Pop. Biol. 2:174-208.

887   Kimura M, Ohta T. 1969. The average number of generations until fixation of a mutant gene
888   in a finite population. Genetics 61:763-771.

889   Latter BDH. 1998. Mutant alleles of small effect are primarily responsible for the loss of
890   fitness with slow inbreeding in *Drosophila melanogaster*. Genetics 148:1143-1158.

891   Li W-H. 1987. Models of nearly neutral mutations with particular implications for non-
892   random usage of synonymous codons. J. Mol. Evol. 24:337-345.

893   Mafessoni F, Lachmann D. 2015. Selective strolls: fixation and extinction in diploids
894   are slower for weakly selected mutations than for neutral ones. Genetics 201:1581-
895   1589.

896   Malécot G. 1969. The Mathematics of Heredity. San Francisco, CA: W.H. Freeman.

897   Maruyama T. 1972. The average number and the variance at a particular gene frequency in
898   the course of fixation of a mutant gene in a finite population. Genet. Res. 19:109-114.

899   Maruyama T, Kimura M. 1974. A note on the speed of gene frequency changes in reverse
900   directions in a finite population. Evolution 28:161-163.

901   McVean GAT, Charlesworth B. 1999. A population genetic model for the evolution of
902   synonymous codon usage: patterns and predictions. Genet. Res. 74:145-158.

903   Nordborg M, Charlesworth B, Charlesworth D. 1996. The effect of recombination on
904   background selection. Genet. Res. 67:159-174.

905   Ohta T. 1971. Associative overdominance caused by linked detrimental mutations. Genet.
906   Res. 18:277-286.

907   Palsson S. 2001. The effects of deleterious mutations in cyclically parthenogenetic organisms. J.
908   Theor. Biol. 208:201-214.

909   Palsson S, Pamilo P. 1999. The effects of deleterious mutations on linked neutral variation in
910   small populations. Genetics 153:475-483.

911   Pamilo P, Palsson S. 1998. Associative overdominance, heterozygosity and fitness. Heredity
912   81:381-389.

913   Roze D. 2015. Effects of interference between selected loci on the mutation load, inbreeding
914   depression and heterosis. Genetics 201:745-757.

915   Roze D, Rousset F. 2004. Joint effects of self-fertilization and population structure on mutation load,
916   inbreeding depression and heterosis. Genetics 167:1001-101.

917   Schou MF, V. L, Bechsgaard J, Schlötterer C, Kristensen TN. 2017. Unexpected high
918   diversity in small populations suggests maintenance by associative overdominance.
919   Mol. Ecol. 26:6510-6523.

920   Sved JA. 1968. The stability of linked systems of loci with a small population size. Genetics
921   59:543-563.

922   Tajima F. 1990. Relationship between DNA polymorphism and fixation time. Genetics
923   125:447-454.

924   Waller DM. 2021. Addressing Darwin's dilemma: Can pseudo-overdominance explain
925   persistent inbreeding depression and load? Evolution 75:779-793.

926   Wang J, Hill WG. 1999. Effect of selection against deleterious mutations on the decline in
927   heterozygosity at neutral loci in closely inbreeding populations. Genetics 153:1475-
928   1489.

929   Wiehe THE, Stephan W. 1993. Analysis of a genetic hitchiking model and its application to
930   DNA polymorphism data. Mol. Biol. Evol. 10:842-854.

931   Zhao L, Charlesworth B. 2016. Resolving the conflict between associative
932   overdominance and background selection. Genetics 203:1315-1334.

933   Zhao L, Lascoux M, Overall ADJ, Waxman D. 2015. The characteristic trajectory of a fixing allele:
934   A consequence of fictitious selection that arises from conditioning. Genetics 195:993-1006

935

936   **Appendix**

937   **Sojourn time formulae**

938   Equation (4.52) of Ewens (2004) can be used to evaluate the sojourn time density conditional on

939   fixation for an allele A_2 at frequency whose initial frequency is $q = 1/N_H$, so that $x \geq q$. This

940   equation can be rewritten as:

941

942     $$t^*(x, q) = 2P_1(x)[x(1-x)\psi(x)]^{-1} \int_x^1 \psi(y) \, dy \qquad \text{(A1a)}$$

943

944   where $P_1(x)$ is the probability of fixation from frequency x, respectively, which is given by:

945

946     $$P_1(x) = \int_0^x \psi(y) \, dy / \int_0^1 \psi(y) \, dy \qquad \text{(A1b)}$$

947

948     $$\psi(y) = \exp - 2 \int \frac{\Delta y}{y(1-y)} \, dy \qquad \text{(A1c)}$$

949

950   Similarly, the probability of loss from frequency x is given by:

951

952     $$P_0(x) = \int_x^1 \psi(y) \, dy / \int_0^1 \psi(y) \, dy \qquad \text{(A1d)}$$

953

954   (Ewens 2004, Equations 4.15-4.17).

955   Substituting the expression for Δx given by Equation (1) of the main text into Equation

956   (A1c) we have:

957     $$\psi(y) = \exp - \gamma(2ay + by^2]) \qquad \text{(A2)}$$

958

959   For $b = 0$ (semi-dominance) analytic expressions for the integrals in Equations (A1) are

960   available (Ewens 2004, pp.165, 169 -170). In other cases, numerical evaluations are needed if the

961   approximations derived below are to be avoided. For this purpose, it is convenient to use series

962   representations of the integrals in Equations (A1b) and (A1c). Expanding the exponential function

963   in Equation (A2), the indefinite integral of $\psi(y)$ can be written as:

964

965     $$\int \psi(y) \, dy = 1 + \sum_{i=1}^{\infty} \frac{(-\gamma)^i}{i!} \int (2ay + by^2)^i \, dy \qquad \text{(A3a)}$$

966

967   With $b \neq 0$, and writing $c = a/b$, this expression can be reduced to a simpler form by the

968   transform $z = (y + c)\sqrt{|\gamma b|}$, which gives $\psi(y)\mathrm{d}y = \exp(\gamma ac)\exp(-z^2)\,\mathrm{d}z/\sqrt{|\gamma b|}$ if $\gamma b > 0$ and

969    $\exp(\gamma ac)\exp(z^2)\,\mathrm{d}z/\sqrt{|\gamma b|}$ if $\gamma b < 0$. The terms in $\exp(-z^2)$ or $\exp(z^2)$ can then be expanded as

970   a Taylor series in z, and integrated term by term to yield an infinite series in z:

971

$$\sqrt{|\gamma b|} \int \psi(y)\,\mathrm{d}y = \exp(\gamma ac) \sum_{i=0}^{\infty} \frac{(-1)^i z^{2i+1}}{(2i+1)!} \qquad (\gamma b > 0) \qquad \text{(A3b)}$$

$$\sqrt{|\gamma b|} \int \psi(y)\,\mathrm{d}y = \exp(\gamma ac) \sum_{i=0}^{\infty} \frac{z^{2i+1}}{(2i+1)!} \qquad (\gamma b < 0) \qquad \text{(A3c)}$$

974

975   If third- and higher-order terms in γ in Equations (A1) - (A3a) are neglected, the following

976   approximations for the components of Equations (A1) emerge after some algebra:

977

$$\psi(x)^{-1} \approx 1 + \gamma(2ax + bx^2) + \gamma^2(2a^2x^2 + 2abx^3 + \tfrac{1}{2}b^2x^4) \qquad \text{(A4a)}$$

979

$$\int_0^x \psi(y)\,\mathrm{d}y \approx x\left[1 - \gamma\left(ax + \tfrac{1}{3}bx^2\right) + \gamma^2\left(\tfrac{2}{3}a^2x^2 + \tfrac{1}{2}abx^3 + \tfrac{1}{10}b^2x^4\right)\right] \qquad \text{(A4b)}$$

981

$$\int_0^1 \psi(y)\,\mathrm{d}y^{-1} \approx 1 + \gamma\left(a + \tfrac{1}{3}b\right) + \gamma^2\left(\tfrac{1}{3}a^2 + \tfrac{1}{6}ab + \tfrac{1}{90}b^2\right) \qquad \text{(A4c)}$$

983

$$\int_x^1 \psi(y)\,\mathrm{d}y \approx (1 - x)\{1 - \gamma\left[a(1 + x) + \tfrac{1}{3}b(1 + x + x^2)\right] + \gamma^2\left[\tfrac{2}{3}a^2(1 + x + x^2) + \right.$$

$$\left. \tfrac{1}{2}ab(1 + x + x^2 + x^3) + \tfrac{1}{10}b^2(1 + x + x^2 + x^3 + x^4)\right]\} \qquad \text{(A4d)}$$

986

987   Inserting these expressions into Equation (A1a), and neglecting higher-order terms in γ, we

988   obtain:

$$t^*(x, q) \approx 2\{1 - \tfrac{1}{3}\gamma bx(1 - x) - \tfrac{1}{3}\gamma^2 x(1 - x)[a^2 + \tfrac{1}{2}ab(1 + 2x)$$

$$+ \tfrac{1}{30}b^2(1 + x[2 + 13x])]\} \qquad \text{(A5)}$$

990

991   For the sojourn time density conditional on loss, Equation (4.52) of Ewens (2004) can be

992   used:

$$t^{**}(x, q) = 2[\int_x^1 \psi(y)\,\mathrm{d}y]^2 P_1(q)[P_0(q)x(1 - x)\psi(x)\int_0^1 \psi(y)\,\mathrm{d}y]^{-1} \quad \text{(A6)}$$

994

995   Using the procedure applied to $t^*(x, q)$, the following second-order approximation with

996   respect to γ is obtained:

997

998     $$t^{**}(x, N_H^{-1}) \approx 2N_H^{-1}(1-x)x^{-1}\{1 - \tfrac{1}{3}\gamma bx(2-x) - \tfrac{1}{3}\gamma^2 x[a^2(2-x) + ab(1 + x[1-x])]$$

999     $$+ \tfrac{1}{30}b^2(x + [2-3x][1-3x] + 13x^2[1-x])]\} \qquad (A7)$$

1000

1001   An approximation for the density function for the expected sojourn time between loss or

1002   fixation at frequency x for a new mutation can similarly be obtained from Equation (4.23) of Ewens

1003   2004):

1004 $$t(x, N_H^{-1}) \approx 2N_H^{-1} \int_x^1 \psi(y)\, dy\, [x(1-x)\psi(x) \int_0^1 \psi(y)\, dy]^{-1} \quad (A8)$$

1005

1006   This expression yields:

1007

        $$t(x, N_H^{-1}) \approx 2N_H^{-1}x^{-1}\{1 + \gamma x \left[a - \tfrac{1}{3}b(1-2x)\right] - \tfrac{1}{3}\gamma^2 x[a^2(1-2x) + $$

1008

1009 $$\tfrac{1}{2}ab(1 + x[3-5x]) + \tfrac{1}{30}b^2(1 + x[1 + x(21-24x)])]\} \qquad (A9)$$

1010

1011   **Background selection approximation**

1012   In this case, only losses of new mutations to the deleterious allele A_2 from a population fixed for the

1013   favorable allele A_1 need to be considered. It is assumed that this process has been going on

1014   indefinitely, and that the population is being observed over a long time period T_o (in units of $2N_e$

1015   generations); the mean diversity at the neutral site is then taken over this period. From Table 1, the

1016   expected number of losses of A_2 over this period is $\lambda_{10}T_o = 0.5\theta_s N_H P_{10} T_o$, and the expected time

1017   interval between successive losses is $T_l = 1/\lambda_{10}$, where $T_l \ll 1$ in the case of BGS. At the start of

1018   this process, which can be assumed to have occurred long before the period of observation, there is

1019   a deviation $\Delta\pi_{2l}$ from 0 of the relative diversity at the end of the first loss event (see Table 1), whose

1020   value can be found by the simulation procedure described in the main text. This is followed by a

1021   recovery period, whose length is drawn from an exponential distribution with rate parameter λ_{10}, so

1022   that the new expected value of $\Delta\pi$ at the end of the recovery period is:

1023

1024 $$\Delta\pi_{2l}^* = \Delta\pi_{2l}\lambda_{10} \int_0^\infty \exp[-(1 + \lambda_{10})t)]\, dt = \frac{\Delta\pi_{2l}\lambda_{10}}{(1+\lambda_{10})} \approx \Delta\pi_{2l}\exp(-T_l) \qquad (A10)$$

1025

1026   The sum of the $\Delta\pi$ values over the recovery period is approximately equal to $\Delta\pi_{2l}T_l$, since

1027   most values will be close to $\Delta\pi_{2l}$ due to the short length of this period; a more exact derivation of

1028   this result can be obtained by use of the argument that yielded Equation S22 of Campos and

1029   Charlesworth (2019).

1030   If the change in diversity at each event is small, we can assume additivity of individual

1031   effects in order to obtain the net change after several events. The second loss event thus results in a

1032   deviation before recovery of $\Delta\pi_{2l}^* + \Delta\pi_{2l}$ and a corresponding sum of $\Delta\pi$ over the recovery period

1033   of $(\Delta\pi_{2l}^* + \Delta\pi_{2l})T_l$. Using the argument above, the post-recovery deviation $\approx (\Delta\pi_{2l}^* +$

1034 $\Delta\pi_{2l})\exp(-T_l) = \Delta\pi_{2l}[1 + \exp(-T_l)]\exp(-T_l)$, and the corresponding sum of $\Delta\pi$ values over the

1035   recovery period $\approx \Delta\pi_{2l}[1 + \exp(-T_l)]T_l$. If this process is repeated indefinitely, it can be seen that

1036   the individual post-recovery deviations are given by the product of $\Delta\pi_{2l}\exp(-T_l)$ and the sum of a

1037   geometric series in $\exp(-T_l)$, which converges on:

1038

1039 $$\Delta\pi_{2l}\exp(-T_l)/[1 - \exp(-T_l)] \approx \Delta\pi_{2l}\lambda_{10} \qquad (A11a)$$

1040

1041   Similarly, the sum of the individual deviations over the recovery period converges on:

1042
1043 $$\Delta\pi_{2l}\lambda_{10}T_l = \Delta\pi_{2l} \qquad (A11b)$$
1044

1045

1046   This formula is the same as for the case when there is a complete recovery of diversity after a

1047   loss of A_2. It therefore follows that the net deviation in diversity caused by multiple losses of

1048 A_2 at rate λ_{10} is approximated by:

1049

1050 $$\lambda_{10}(\Delta\pi_{20w} + \Delta\pi_{2l}) \qquad (A12)$$

1051

1052   **Table 1 Parameters used in the model of associative overdominance**

1053

1054 u rate of mutation per generation from A_1 to A_2 at the selected locus

1055 v rate of mutation per generation from A_2 to A_1 at the selected locus

1056 κ mutational bias parameter, such that $u = \kappa v$

1057 θ_s scaled mutation rate at the selected locus, such that $\theta_s = 4N_e u$

1058 P_{10} Probability of loss of an A_2 mutation introduced into a population fixed for A_1.

1059 P_{11} Probability of fixation of an A_2 mutation introduced into a population fixed for A_1.

1060 P_{20} Probability of loss of an A_1 mutation introduced into a population fixed for A_2.

1061 P_{21} Probability of fixation of an A_1 mutation introduced into a population fixed for A_2.

1062 λ_{10} Rate of loss of new A_2 mutations from a population fixed for A_1 (in units of $2N_e$

1063   generations); $\lambda_{10} = 0.5\,\theta_s N_H P_{10}$

1064 λ_{11} Rate of fixation of new A_2 mutations in a population fixed for A_1 (in units of $2N_e$

1065   generations); $\lambda_{11} = 0.5\,\theta_s N_H P_{11}$

1066 λ_{20} Rate of loss of new A_1 mutations from a population fixed for A_2 (in units of $2N_e$

1067   generations); $\lambda_{20} = 0.5\kappa^{-1}\theta_s\,N_H P_{20}$

1068 λ_{21} Rate of fixation of new A_1 mutations in a population fixed for A_2 (in units of $2N_e$

1069   generations); $\lambda_{21} = 0.5\kappa^{-1}\theta_s\,N_H P_{21}$

1070 $\Delta\pi_{il}$ Value of $\Delta\pi$ at the neutral site, when an allele of type A_i has just become lost from the

1071   linked selected site.

1072 $\Delta\pi_{if}$ Value of $\Delta\pi$ at the neutral site, when an allele of type A_i has just become fixed at the

1073   linked selected site.

1074 $\Delta\pi_{i0S}$ Sum of $\Delta\pi$ values at the neutral site over the course of the loss of a type i mutation from the

1075   linked selected site.

1076 $\Delta\pi_{i1S}$ Sum of $\Delta\pi$ values at the neutral site over the course of the fixation of a type i mutation at the

1077   linked selected site.

1078

1079   **Table 2   Comparison of the deterministic BGS predictions for the**

1080   **reduction in neutral diversity with simulations of losses of**

1081   **deleterious mutations from populations fixed for the favorable allele**

h	$u/hs = 0.2$	$u/hs = 0.1$	$u/hs = 0.05$	$u/hs = 0.025$
0.4	$\gamma = 6.25$ 0.124±0.011	$\gamma = 12.5$ 0.089±0.003	$\gamma = 25$ 0.053±0.001	$\gamma = 50$ 0.027±0.001
0.3	$\gamma = 8.33$ 0.130±0.005	$\gamma = 16.6$ 0.084±0.003	$\gamma = 33.3$ 0.050±0.001	$\gamma = 66.6$ 0.027±0.001
0.2	$\gamma = 2.5$ 0.123±0.005	$\gamma = 25$ 0.076±0.002	$\gamma = 50$ 0.035±0.001	$\gamma = 100$ 0.026±0.001
0.1	$\gamma = 25$ 0.102±0.003	$\gamma = 50$ 0.066±0.002	$\gamma = 100$ 0.041±0.001	$\gamma = 200$ 0.024±0.001

1082

1083

1084   The lower entries in each cell are the simulation results for the reductions in neutral diversity

1085   (with standard errors) under recurrent losses of completely linked, deleterious mutant alleles

1086   from a population fixed for the selectively favorable alternative, with mutation rate u to

1087   deleterious alleles, selection coefficient s and dominance coefficient h. The population size is

1088 $N = 500$, so that $s = \gamma/1000$, the scaled deleterious mutation rate is $\theta_s = 4Nu = 1$, and $u = 2.5 \times$

1089 10^{-4}.

1090

1091
1092
1093   Figure 1. Mean times to fixation of a new mutation as a function of the absolute value of

1094   the scaled selection coefficient γ, assuming autosomal inheritance and a Wright-Fisher

1095   model of genetic drift with population size N. Times are in units of coalescent time ($2N$

1096   generations). The cases with negative selection have a dominance coefficient $h = 0.1$ and

1097   those with positive selection have $h = 0.9$. The results for two different values of N are

1098   shown. The red points with error bars are the mean values from simulations and their

1099   standard errors. The blue curves are the values from the approximation of Equation (2), and

1100   the black curves are the values from numerical integrations of the diffusion equation results

1101   (Equations A1). The horizontal lines are the neutral values from the numerical integrations.

1102
1103

1104
1105
1106
1107
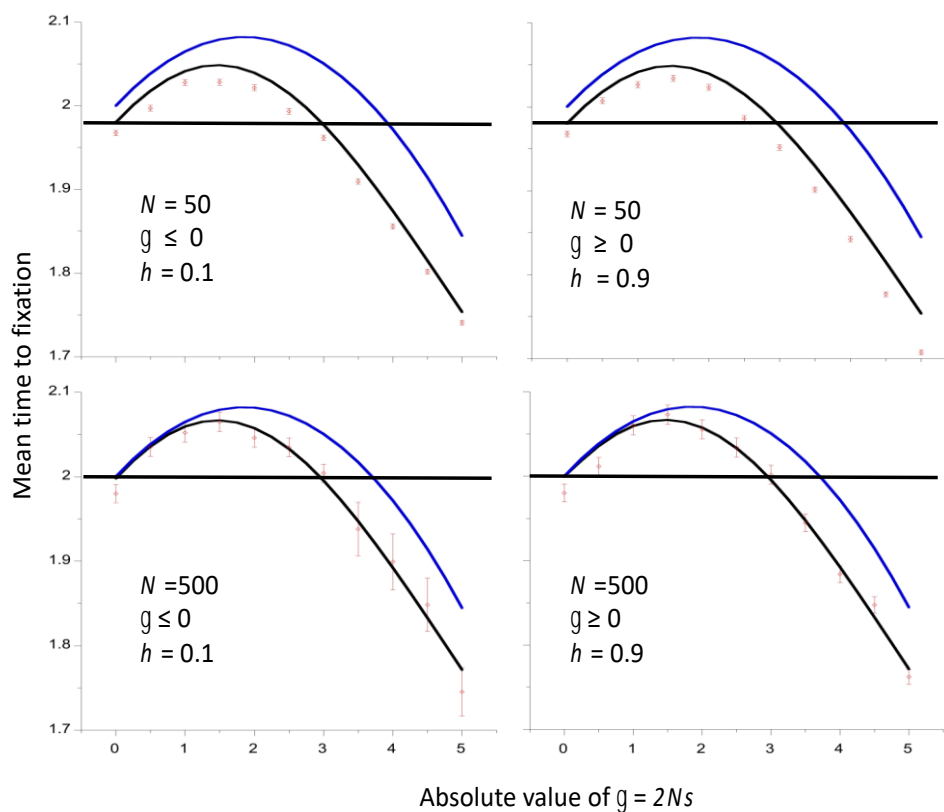
1108

1109

1110   Figure 2. Mean times to loss of a new mutation as a function of the absolute value of the

1111   scaled selection coefficient, assuming autosomal inheritance and Wright-Fisher model of

1112   genetic drift with population size N. Times are in units of coalescent time ($2N$ generations).

1113   The cases with negative selection have a dominance coefficient $h = 0.1$ and those with

1114   positive selection have $h = 0.9$. The results for two different values of the population size, N,

1115   are shown. The red points with error bars show the mean values of simulations and their

1116   standard errors. The blue curves are the values from the approximation of Equation (3), and

1117   the black curves are the values from numerical integrations of the diffusion equation results

1118   (Equations A1 and A6). The horizontal lines are the neutral values from the numerical

1119   integrations.

1120

1121
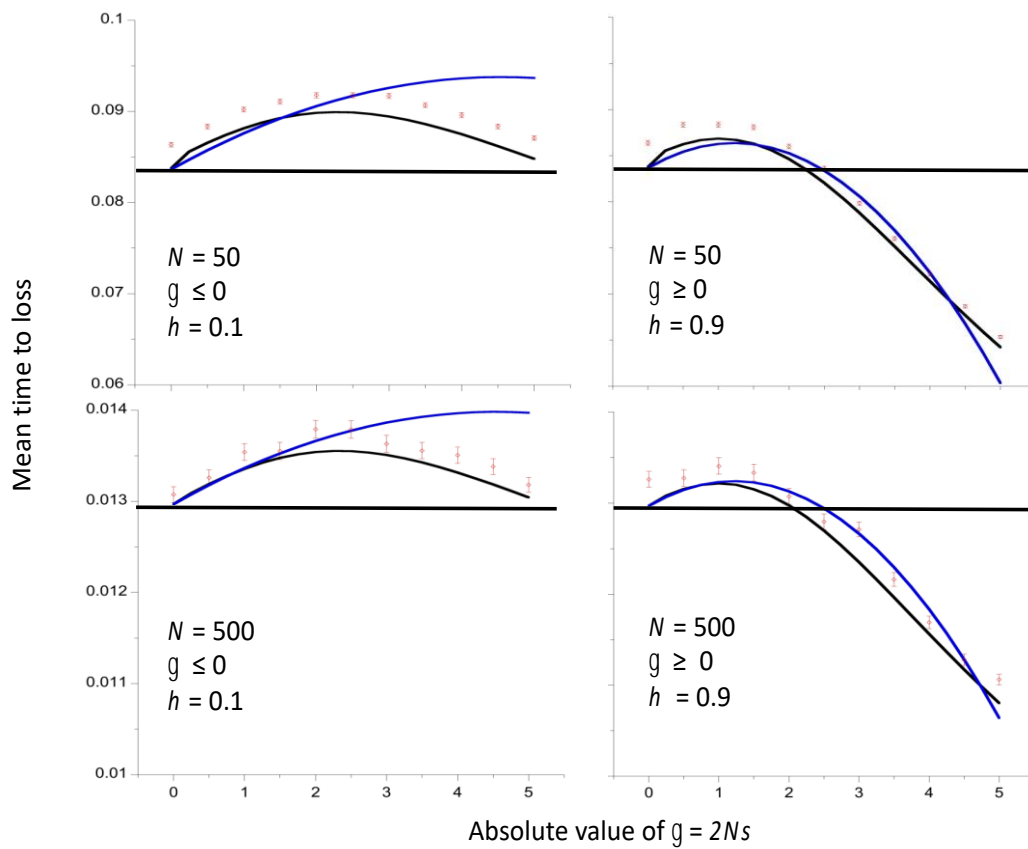
1122
1123

1124
1125

1126

1127   Figure 3. Mean times to fixation and loss of a new mutation (in units of coalescent time) as

1128   functions of the dominance coefficient h , for the models used in Figures 1 and 2. The black

1129   and blue lines are the values from the approximations of Equations (2) and (3), for $|\gamma| = 1$

1130   and 2, respectively. The dashed green and red lines are the corresponding values from

1131   numerical integrations of the diffusion equation expressions. The horizontal lines are the

1132   neutral values from the numerical integrations. The population size N is equal to 500.

1133
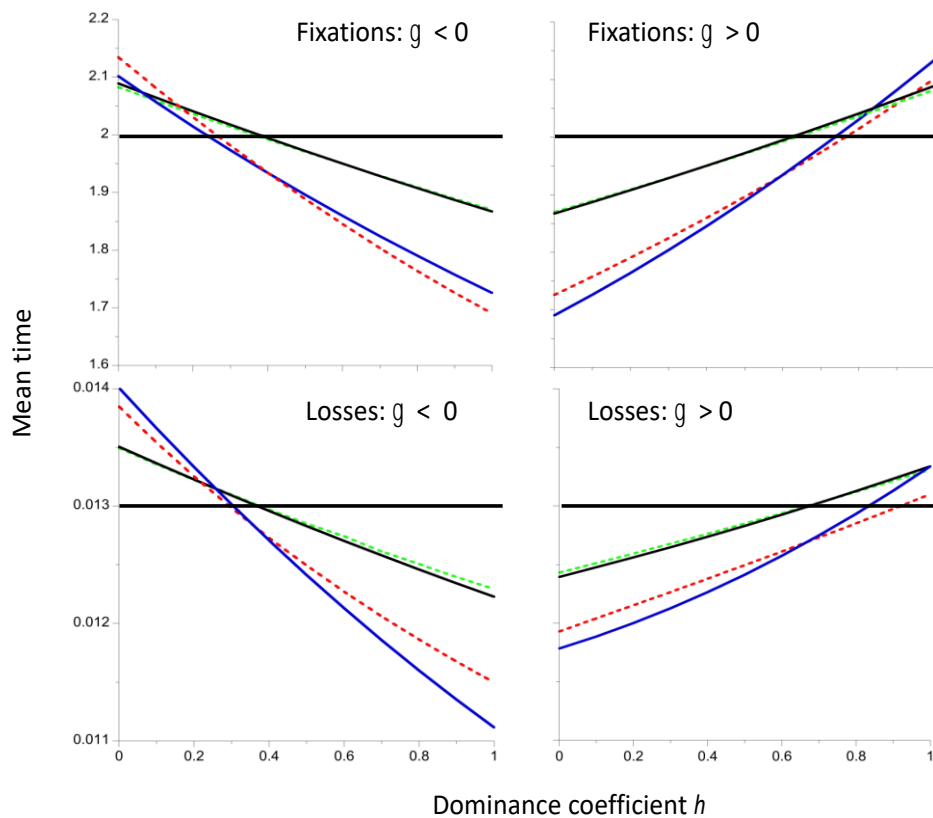
1134
1135

1136

1137

1138   Figure 4. The critical values of the dominance coefficient as functions of the scaled selection

1139   coefficient for mean fixation time (full red line) or mean loss time (dashed black line). The

1140   results were obtained using the approximate Equations (8). The blue curves are the

1141   solutions to Equation (18) of Zhao and Charlesworth (2016). The results for favorable

1142   mutations are shown in the left-hand panel) and those for deleterious mutations in the

1143   right-hand panel

1144

1145

1146
1147

1148

1149
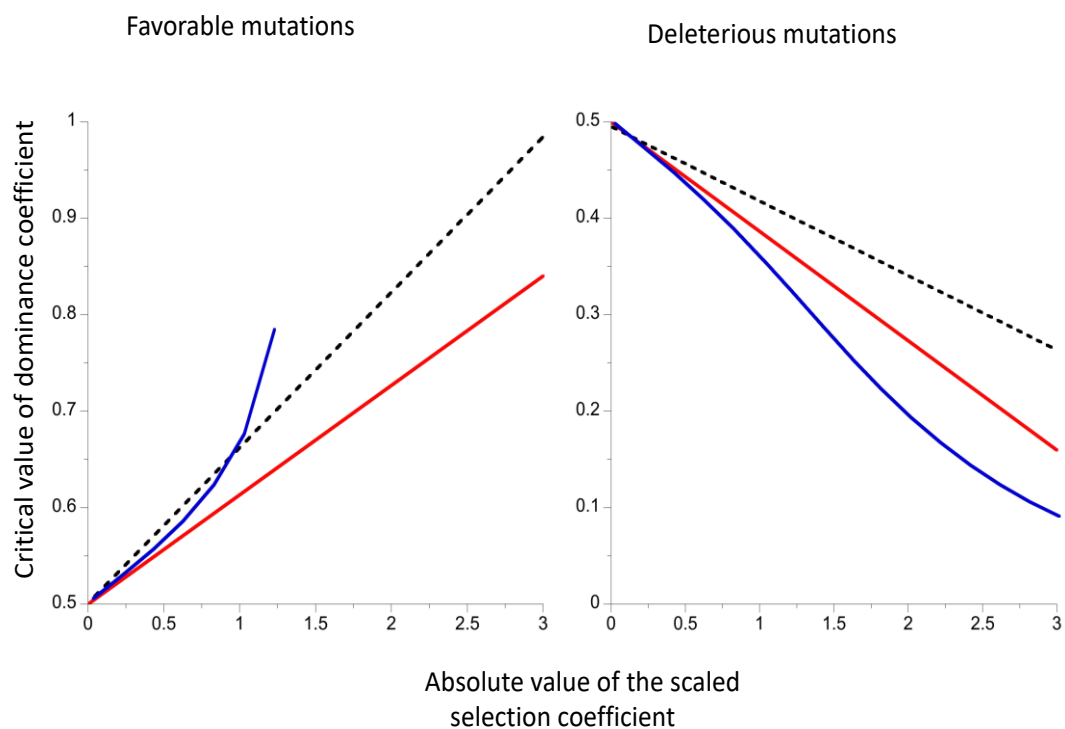
1150   Figure 5. The left-hand panel shows the mean pairwise diversities (relative to the purely

1151   neutral value θ) at a neutral site during the course of fixation of a completely linked

1152   beneficial mutation with dominance coefficient $h = 0.9$, for haplotypes carrying the

1153   ancestral allele (A_1), the new mutation (A_2), and the divergence between A_1 and A_2

1154   haplotypes (A_1 versus A_2). The final diversity at the time of fixation of A_2 and the mean

1155   diversity over all three haplotypes over the course of the fixation process are also shown.

1156   Autosomal inheritance and a Wright-Fisher model of genetic drift with population size $N =$

1157   50 were simulated by the method of Tajima (1990). The right-hand panel displays the mean

1158   values and standard errors of the net change in relative diversity over repeated fixation

1159   events for two different N values, estimated from the simulations by the method described

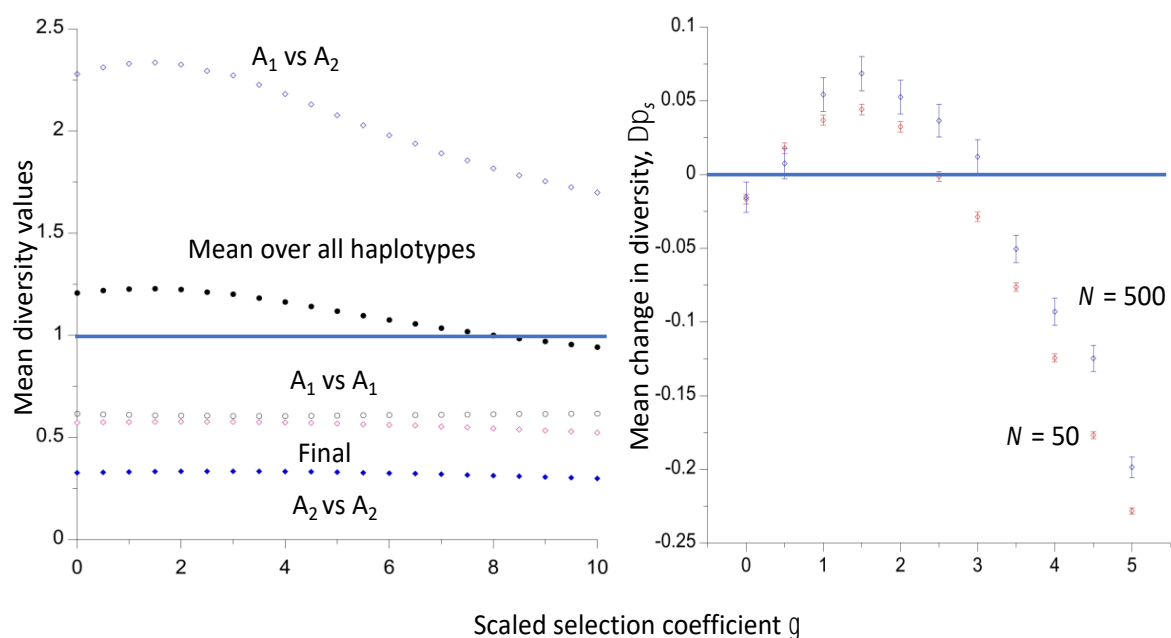1160   in the text.

1161

1162
1163

1164

1165

1166   Figure 6. The mean values and standard errors of the net changes in relative diversity over

1167   repeated loss events with two different N values, for deleterious mutations with $h = 0.1$ and

1168   favorable mutations with $h = 0.9$, using the same model and methods as in Figure 7.

1169

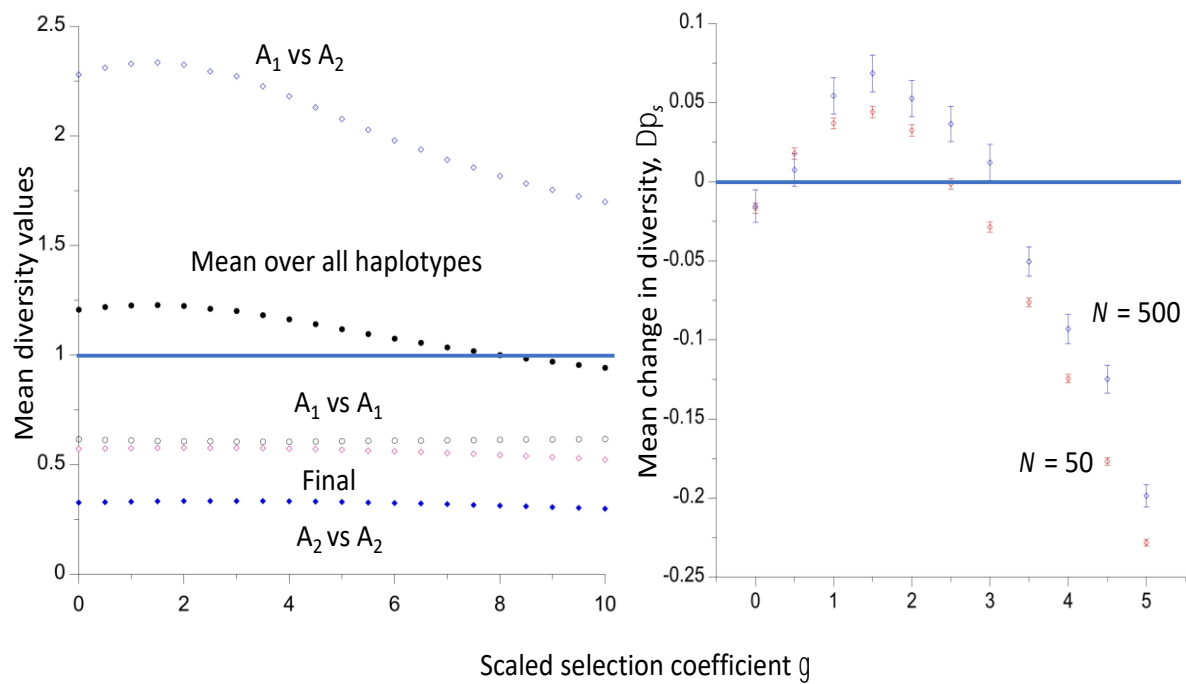1170

1171

1172
1173

1174
1175

1176

1177   Figure 7. The expected deviation of relative diversity for a completely linked neutral site

1178   from its value in the absence of selection ($\Delta\pi_e$), at the stationary state under genetic drift,

1179   mutation and selection. The dominance coefficients for deleterious and favorable mutations

1180   are h = 0.1 and h = 0.9, respectively. Equal frequencies of mutations in each direction at the

1181   selected site were assumed, with a scaled mutation rate θ_s = 0.01. The means and standard

1182   errors over replicate simulations are shown for population sizes of 50 (red points) and 500

1183   (black points).

1184

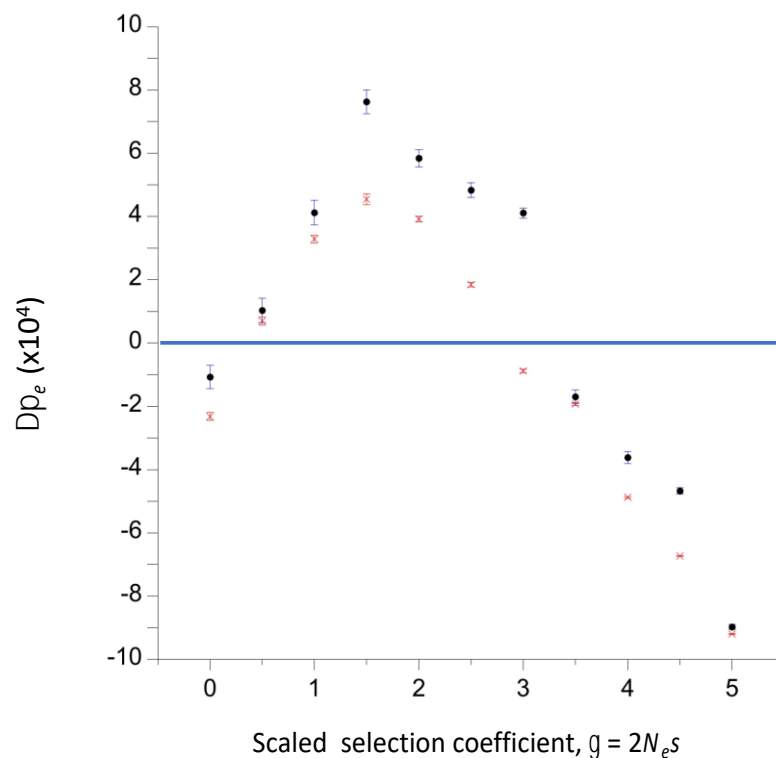1185

1186

1187
1188

1189

1190

1191   Figure 8. The upper two panels show the approximate (full curves) and exact (dashed

1192   curves) sojourn time densities for mutations that become lost, relative to the corresponding

1193   neutral values. The lower two panels are the sojourn time densities for mutations that

1194   become fixed. The left-hand panels are for $|\gamma| = 1$ and the right-hand panels are for $|\gamma| = 2$.

1195   Deleterious mutations with $h = 0.1$ are the red curves and beneficial mutations with $h = 0.9$

1196   are the black curves. The exact results were obtained by numerical integrations of the

1197   relevant equations described in the Appendix; the approximate results were obtained from

1198   Equations (A5) and (A7).

1199

1200

1201

1202

1203

1204